DOI https://doi.org/10.32782/1994-4691-2026-1-77-3
UDK 621.225.001.4

DYNAMIC MODEL OF A HYDRAULIC DRIVE OF A MECHATRONIC SYSTEM WITH A PLANETARY HYDRAULIC MOTOR

ДИНАМІЧНА МОДЕЛЬ ГІДРАВЛІЧНОГО ПРИВОДУ МЕХАТРОННОЇ СИСТЕМИ З ПЛАНЕТАРНИМ ГІДРОМОТОРОМ

A. Panchenko[1], Doctor of Technical Sciences ORCID: 0000-0002-1230-1463
A. Voloshina[1*], Doctor of Technical Sciences ORCID: 0000-0003-4052-2674
I. Panchenko[1], Candidate of Technical Sciences ORCID: 0000-0003-2150-4278
I. Kholod[1], Assistant ORCID: 0000-0002-3652-0687
A. Voloshin[2], Teacher of Specialized Disciplines ORCID: 0009-0004-3850-7613

[1]*Dmytro Motornyi Tavria State Agrotechnological University*
[2]*Melitopol Vocational College of TSATU*
*e-mail: voloshinaa2012@gmail.com

Abstract. This paper summarizes computational studies of the dynamic characteristics of a mechatronic hydraulic drive with standard and modernized planetary hydraulic motors. The aim is to compare the effects of motor design, external disturbances and passive pulsation damping on the transient response of the drive. The analysis considers the flow area of the distribution system, the diametral clearance between the rotors, pump delivery variations and changes in resisting torque. Three cases are examined: constant pump delivery and resisting torque, variable external inputs, and operation with a passive pulsation damper. Variations in the distribution flow area are associated with pressure and flow rate pulsations, while variations in the diametral clearance are associated with torque oscillations. Under variable external inputs, the modernized motor exhibits smaller pressure and torque oscillations and reaches the operating speed level earlier than the standard motor. In the case with a passive pulsation damper of 5000 cm³, the approximate start-up pressure peaks are 38 and 36 MPa for the standard and modernized motors, respectively, compared with 90 and 85 MPa without the damper. The start-up torque peaks are within 900–1000 N·m for both designs, compared with approximately 2100 and 1900 N·m without the damper. However, oscillations under variable loading remain in both designs. The results support considering motor design improvements and passive damping together when selecting measures to reduce pulsations and start-up loads. The numerical estimates apply to the cases considered, taking into account differences in their initial parameters and operating conditions.

Keywords: transient processes, hydraulic drive acceleration, pressure, torque, working fluid flow rate, rotational speed.

Introduction.

Modern mechatronic systems of self-propelled machinery are subject to increased requirements for response speed, accuracy, energy efficiency and stability of operating processes. Many actuating mechanisms in such machines are based on hydraulic drives capable of providing high torque with relatively small dimensions and low weight. The dynamic characteristics of the hydraulic drive directly determine the operating performance of the mechatronic system, particularly during start-up, load changes and other transient conditions [1, 2].

Planetary hydraulic motors are a promising type of hydraulic actuator for mechatronic systems of self-propelled machinery, combining compactness, high specific torque and the ability to operate under substantial loads. Their design features result in a complex process of working volume formation and torque transmission to the output shaft. The design features of

the rotor system, particularly the diametral clearance [2, 3], and the distribution system, particularly variations in the flow area [4–6], have a significant effect on operating characteristics.

The study of dynamic processes occurring in hydraulic drives of mechatronic systems of self-propelled machinery is of particular importance. Pressure, flow rate and torque pulsations may reduce motion stability, increase dynamic loads and vibration, and shorten the service life of hydraulic drive components [2, 7]. The dynamics of the hydraulic drive are determined by the interaction of the pump, pipelines, control and safety devices, hydraulic motor and external mechanical load [8]. For a planetary hydraulic motor, periodic processes in the rotor system [2, 9] and the distribution system [5, 7, 10] are an additional source of disturbances. Changes in the geometry of the working ports affect flow capacity and pressure pulsations, while the parameters of the rotor system, including the diametral clearance, affect the generation of output torque [3, 9]. However, the combined effect of these factors on hydraulic drive dynamics under simultaneous operating disturbances remains insufficiently understood. This particularly concerns the quantitative assessment of the relationship between hydraulic motor design modifications, pressure and flow rate pulsations, torque variations and relief valve operation.

The use of passive damping devices also requires further study. Hydropneumatic accumulators and other smoothing devices are known to reduce the amplitude of hydraulic pulsations [11, 12]. However, their effectiveness in a hydraulic drive with a planetary hydraulic motor should be assessed taking into account the transient response of the entire system. In particular, it is of interest to compare start-up pressure and torque peaks, as well as subsequent oscillations of the output parameters, in the computational cases considered without a damper and with a passive pulsation damper.

Thus, it is relevant to systematize the research results on the effects of planetary hydraulic motor design parameters, uneven pump delivery, external load variations and passive damping on the dynamic characteristics of the hydraulic drive. This synthesis makes it possible to compare the potential of hydraulic motor design modifications and the use of a pulsation damper, taking into account differences in the initial parameters and conditions of the computational cases considered.

Literature Review.

Current research on planetary and orbital hydraulic motors can broadly be divided into several interrelated areas: improvement of rotor and distribution systems, investigation of hydraulic motor output characteristics and dynamics, modeling of pressure and flow rate pulsations, development of methods for their suppression, and investigation of the dynamics of control and safety devices. Analysis of these areas shows that most existing studies consider individual components or individual operating modes of the hydraulic drive, while comprehensive investigation of the interaction between design and operating factors remains insufficiently developed.

Approaches to the mathematical description of mechatronic systems with hydraulic drives have been proposed [1]. An important advantage of this study is the possibility of linking the parameters of individual components to the characteristics of the system as a whole. However, the main attention is given to the development of mathematical and kinematic models, while operating disturbances and their interaction with the hydraulic motor's own dynamic processes receive limited consideration.

A substantial proportion of research is devoted to improving the output characteristics of planetary hydraulic machines. The influence of tooth curvature radius on the geometric and functional parameters of rotors has been investigated [9], and a design for a planetary gear mechanism has been proposed [13]. These results confirm the high sensitivity of hydraulic motors to the geometric parameters of their working elements. However, the main findings primarily concern the assessment of output or geometric characteristics, while the dynamic

consequences of changes in these parameters for the entire hydraulic drive receive less attention. Thus, an improvement in static characteristics alone does not yet indicate an improvement in the dynamic stability of the system.

Studies of the diametral clearance are of particular importance to the problem under consideration [3]. The results show that changes in the clearance can significantly affect the operating characteristics of the hydraulic machine. An increase in clearances is also associated with changes in internal leakage and the process of torque generation. Therefore, the diametral clearance should be considered not only as a parameter of reliability and manufacturing accuracy, but also as a factor determining the dynamic behavior of the hydraulic drive.

Another important area is the study of distribution systems. The results show that the geometry of the working ports, variations in the flow area [4, 5], and the manufacturing accuracy of the components of the planetary hydraulic motor's end-face distribution system [10] directly affect flow capacity. Together with the research findings, this provides a basis for considering the distribution system as one of the main sources of periodic disturbances in the hydraulic motor. However, research mainly focuses on flow capacity as a characteristic of the distribution system, while its relationship with the pressure and torque time histories within a closed dynamic system is not considered in sufficient detail. The combined effect of the design features of the distribution system and the rotor mechanism is also not fully understood, although their periodic interaction generates a substantial proportion of the internal disturbances in the planetary hydraulic motor.

The dynamic behavior of mechatronic systems with planetary hydraulic motors has been investigated [2, 7]. The combined effect of hydraulic motor design features and operating disturbances is considered in [8], while the use of a passive pulsation damper to reduce start-up dynamic loads is considered in [14]. These studies are directly related to the problem under consideration and demonstrate the need to account for transient processes occurring in the hydraulic drive of a mechatronic system of self-propelled machinery. However, further development in this area requires a more detailed distinction between the sources of disturbances. In particular, it is insufficient to consider the transient process solely as a result of a change in the operating mode of the hydraulic drive: the effects of the rotor and distribution systems, pump pulsations and external load need to be assessed separately. Without this distinction, it is difficult to determine which design parameter is decisive for a particular dynamic characteristic.

A broader body of research is devoted to the dynamics of hydrostatic drives. The dynamic processes of a low-speed, high-torque hydrostatic drive have been investigated [15]; a mathematical model and analysis of a hydrostatic transmission have been presented [16]; a CFD model of internal leakage flow in a radial piston hydraulic motor has been developed [17]; the reliability of a mathematical model of transient processes in the hydraulic drive of a mechatronic system has been assessed [18]; a dynamic analysis of a hydraulic drive has been performed through modeling and simulation [19]; and the dynamic characteristics of a hydraulic motor operating under pulsating flow have been investigated [20]. A common advantage of these studies is that they consider the hydraulic drive as an interconnected hydromechanical system. However, the objects and problems considered do not fully correspond to the specific features of a planetary hydraulic motor. As a rule, these studies do not account for the periodic formation of the working volume and flow distribution characteristic of the hydraulic machine under consideration.

A separate research area concerns pulsations of speed, delivery and pressure. In [21], a model of rotational speed pulsations in a high-torque hydraulic motor is proposed, taking into account the effects of friction and leakage at the interfaces between its components. These results demonstrate the need to consider internal hydraulic motor processes when analyzing motion irregularity. For the hydraulic drive under consideration, it is of interest to compare these internal factors with external effects, namely uneven pump delivery and load variations.

Dynamic modeling of a pneumatic radial piston motor has been performed [22]; pulsations of the delivery flow of a piston pump have been investigated [23]; active control of pressure pulsations in an axial piston pump has been analyzed [24]; a mathematical model of pressure pulsations in a hydrostatic transmission has been developed [25]; pressure ripple characteristics in hydraulic circuits have been simulated [26]; and models of hydropneumatic accumulators and their applications in hydraulic systems, including hydraulic shock absorption and pulsation damping, have been reviewed [27]. Methods for modeling a passive hydraulic damper [12], as well as methods for suppressing pressure pulsations in hydraulic systems, have been proposed. The classification and characteristics of pulsation dampers have been considered [11]. Despite the wide range of proposed solutions, a significant limitation of most studies is that the effectiveness of damping devices is assessed mainly by the reduction of pulsations in the hydraulic circuit. This is insufficient for hydraulic drives of mechatronic systems of self-propelled machinery, since a reduction in pressure does not necessarily produce a proportional reduction in torque oscillations or shorten the transient time.

The relief valve is an important component affecting the transient process. The mathematical foundations of dynamic modeling have been presented [28], and mathematical modeling and dynamic analysis of processes occurring in a hydraulic system with a relief valve have been performed [29]. These studies show that the valve is a dynamic component rather than an ideal device that limits pressure instantaneously. However, most of the models considered focus on the valve itself or a local hydraulic circuit. Its effect on the dynamics of a drive whose actuator is a planetary hydraulic motor with a pronounced periodic operating process remains insufficiently studied.

Previous studies have considered the effects of the design features of the rotor system [2] and the distribution system [7] of a planetary hydraulic motor on the dynamic characteristics of the hydraulic drive. The combined effect of hydraulic motor design features and operating disturbances [8], as well as the use of a passive pulsation damper to reduce start-up pressure and torque surges [14], has been investigated. These results form the basis of the present synthesis. Their systematization makes it possible to compare the potential of hydraulic motor design modifications and passive damping under different hydraulic drive operating conditions.

The aim of this work is to summarize and compare the results of previous simulations of the dynamic characteristics of the hydraulic drive of a mechatronic system with standard and modernized planetary hydraulic motors, considering the effects of design parameters, uneven pump delivery, external load variations and the use of a passive pulsation damper. The main focus is on the reduction of start-up pressure and torque surges, the reduction of pulsations, and changes in acceleration duration, taking into account the initial conditions of the computational cases considered.

Research Methodology.

To achieve the stated aim of summarizing and comparatively assessing previously obtained results, the following tasks are addressed:

– to systematize the input data and conditions of previous simulations that determine the specific features of the computational cases considered;

– to summarize the mathematical relationships and structural and functional diagrams used to describe dynamic processes in the hydraulic drive of a mechatronic system with a planetary hydraulic motor;

– to compare the results of studies on the effects of the design features of the rotor and distribution systems of standard and modernized hydraulic motors on the dynamic characteristics of the hydraulic drive;

– to analyze previously obtained results, taking into account uneven pump delivery and external load variations;

– to compare start-up pressure and torque peaks and the patterns of variation in output

parameters in computational cases without and with a passive pulsation damper, taking into account the initial simulation conditions.

The relationships presented in [30] are used to describe the structure of the mathematical model of the hydraulic drive of a mechatronic system with a planetary hydraulic motor. They describe variations in output characteristics, taking into account the geometric parameters of the hydraulic motor, the movement of rotor system components and changes in the flow area of the distribution system. The present work summarizes the results of applying mathematical models to analyze hydraulic motor design features, operating disturbances and passive damping [2, 7, 8, 14].

The sequence of reviewing and comparing the results is shown in Fig. 1. It covers the effects of the design features of the rotor and distribution systems of the planetary hydraulic motor, external disturbances, namely uneven pump delivery and load fluctuations, and the use of a passive pulsation damper.

First, the results of separate investigations into the effects of the diametral clearance in the rotor system [2] and variations in the flow area of the distribution system [7] on the dynamic characteristics of the hydraulic drive are considered. Next, the results of investigating their combined effect in the presence of operating disturbances [8] and the results of using a passive pulsation damper [14] are analyzed. The comparison takes into account the initial parameters and simulation conditions of each computational case.

In the studies considered [2, 7, 8], transient processes in the hydraulic drive of the mechatronic system were simulated for a planetary hydraulic motor with a displacement of V_{hm0} = 160 cm³. The VisSim simulation package was used to determine the effects of the design features of the rotor and distribution systems on the dynamic characteristics of the hydraulic drive.

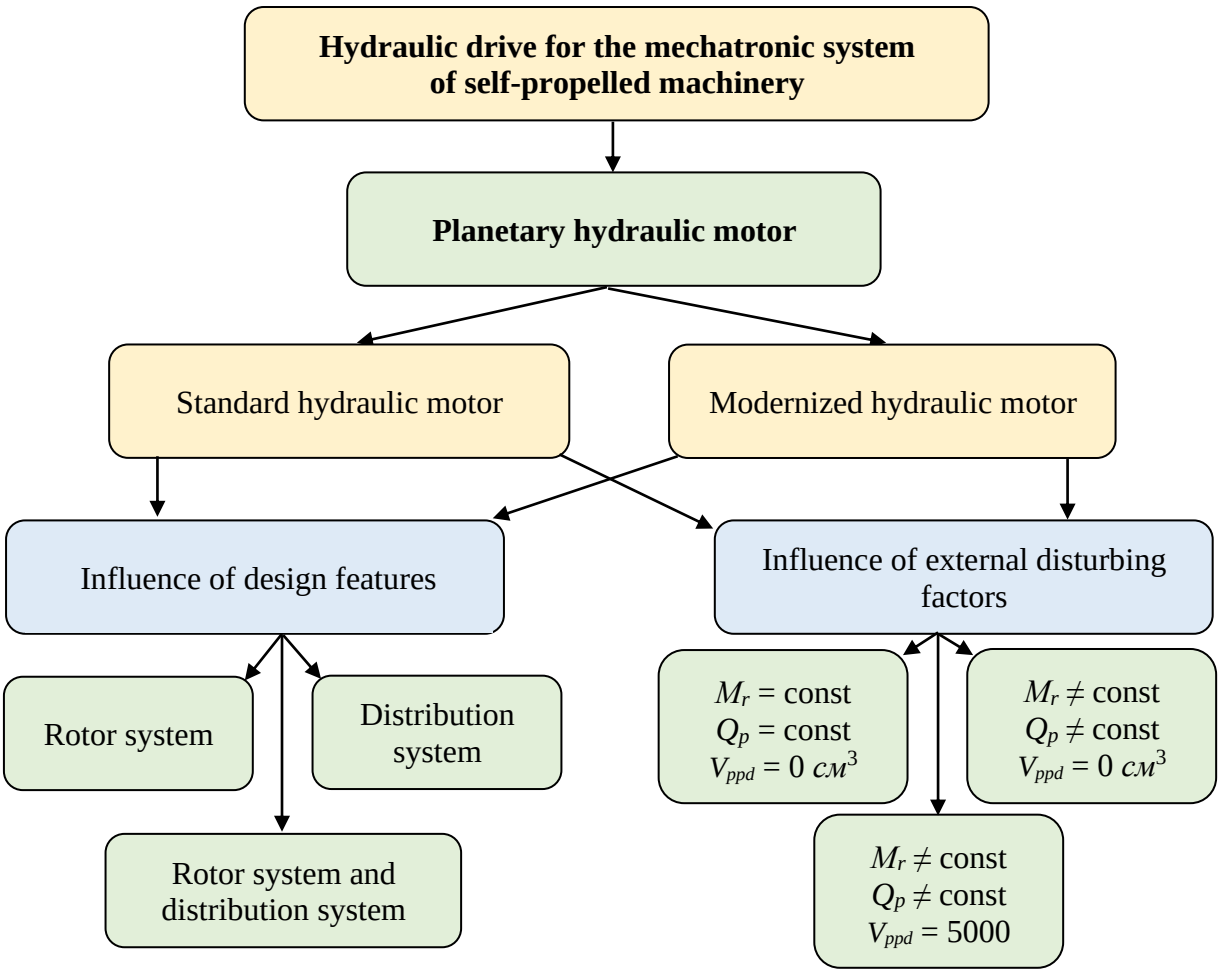


Fig. 1. Research scheme for the dynamic characteristics of a planetary hydraulic motor operating as part of the hydraulic drive of a mechatronic system of self-propelled machinery

Simulations were performed for standard and modernized planetary hydraulic motors. The structural and functional blocks of the dynamic model are presented below (Figs. 2–12), explaining the relationships used and the procedure for setting the parameters. The initial conditions of individual computational cases are considered when analyzing the corresponding results.

The input data are specified in block **A** of the structural and functional diagram of the dynamic model of the hydraulic drive of a mechatronic system with a planetary hydraulic motor (Fig. 2).

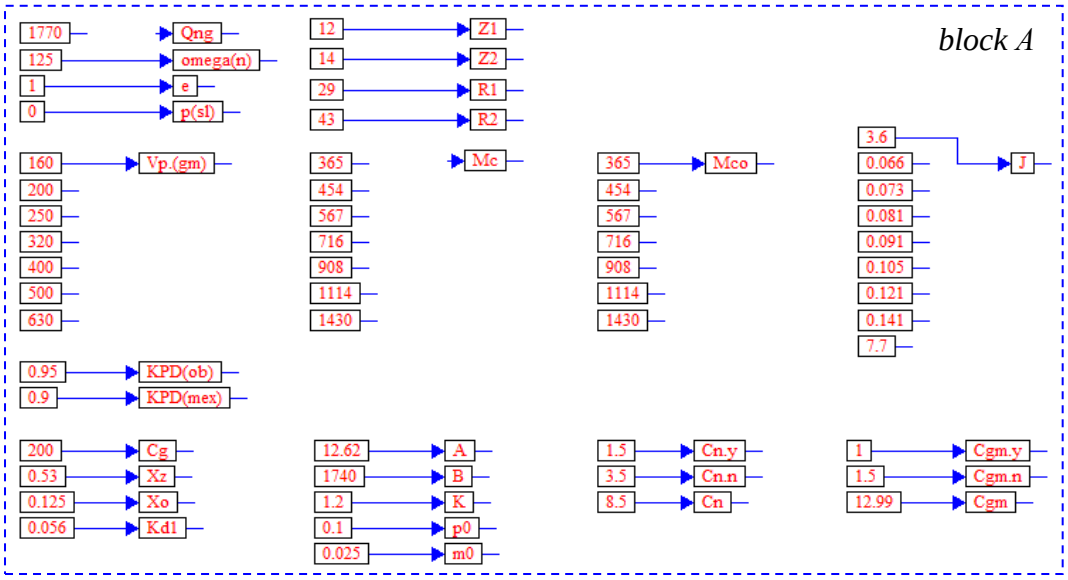


Fig. 2. Input data for the dynamic model

Block **B** (Fig. 3) allows the rotation of the movable distributor to be simulated and the relative angular positions of the ports of the movable and stationary distributors to be determined using the relationships [4, 5]:

– for the movable distributor:

$$\alpha = \frac{2\pi}{Z_1},\ \alpha_1(t) = \int \omega_{hm} dt,\ \alpha_2(t) = \alpha_1(t) + \alpha,\ \ldots,\ \alpha_i(t) = \alpha_{i-1}(t) + \alpha, \quad (1)$$

where Z_1 is the number of ports in the movable distributor;

– for the stationary distributor:

$$\beta = \frac{2\pi}{Z_2},\ \beta_1 = \frac{\pi}{Z_2},\ \beta_2 = \beta_1 + \beta,\ \ldots,\ \beta_i = \beta_{i-1} + \beta, \quad (2)$$

where Z_2 is the number of ports in the stationary distributor.

Block **B** also allows the angle defining the geometric limits of the distribution ports to be determined using the following relationship:

$$\varepsilon = \frac{\pi}{Z_2} - \delta, \quad (3)$$

where δ is the angular clearance between the ports of the movable and stationary distributors.

Block **C** (Fig. 4) allows the angular distance between the centers of the overlapping ports of the movable and stationary distributors during rotation of the movable distributor to be determined using the following expression:

$$\sigma_i(t) = |\beta_i - \alpha_i(t)|. \quad (4)$$

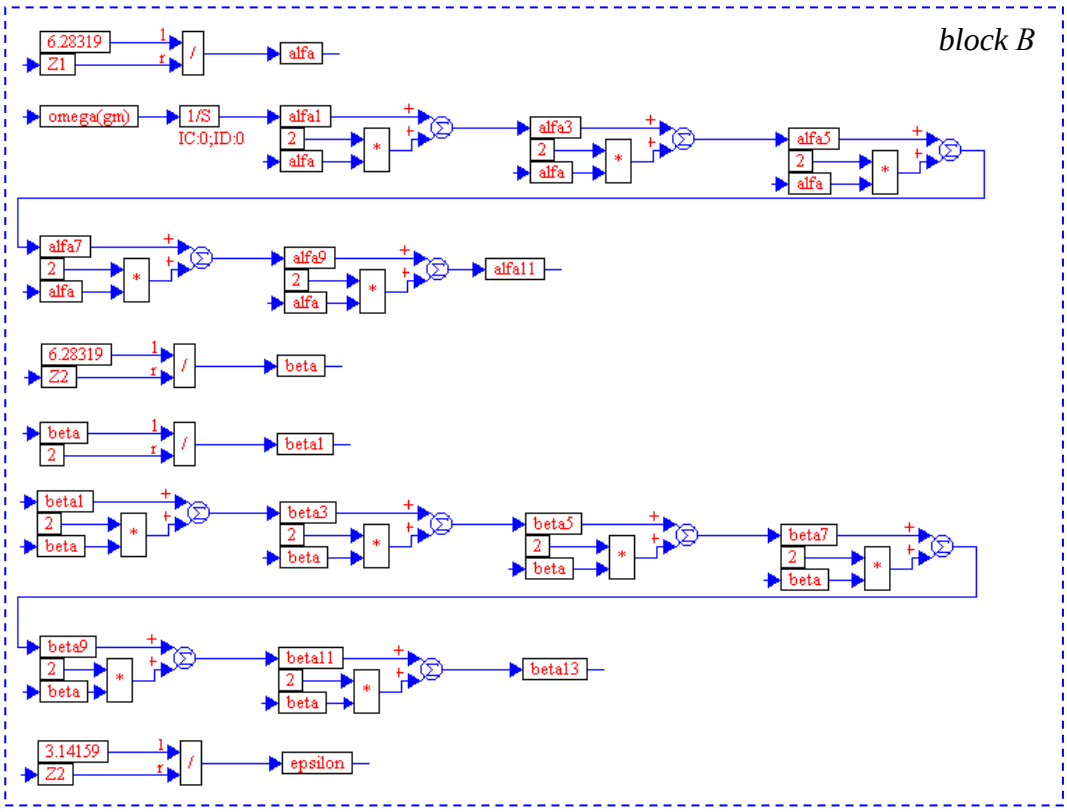


Fig. 3. Dynamic model block for determining the angular positions of the distribution ports of the movable and stationary distributors

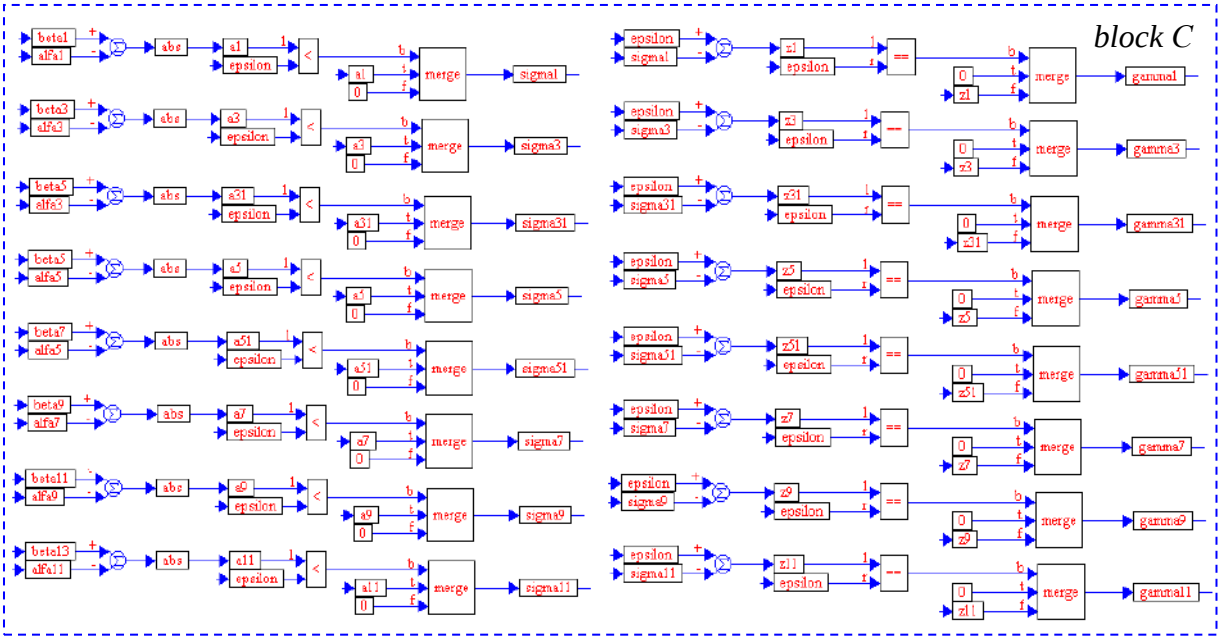


Fig. 4. Dynamic model block for determining the distance between the centers of the ports of the movable and stationary distributors and their overlap angles

It also allows the overlap angles of the pressure ports of the stationary distributor with each port of the movable distributor to be determined using the following expression:

$$\gamma_i(t) = \varepsilon - \sigma_i(t). \quad (5)$$

Block **D** (Fig. 5) allows the overlap area of the pressure ports of the stationary distributor with each port of the movable distributor to be determined as a function of time using the following expression [4–6]:

$$A_i(t)=\sum_{i=1}^{Z}\left(\frac{\pi}{Z_2}-\delta-\left|\beta_i-\alpha_i(t)\right|\right)\cdot\frac{\left(R_2^{02}-R_1^{02}\right)}{2}, \quad (6)$$

where $R_1{}^0$ and $R_2{}^0$ are the inner and outer radii defining the lower and upper boundaries of the distribution ports, respectively.

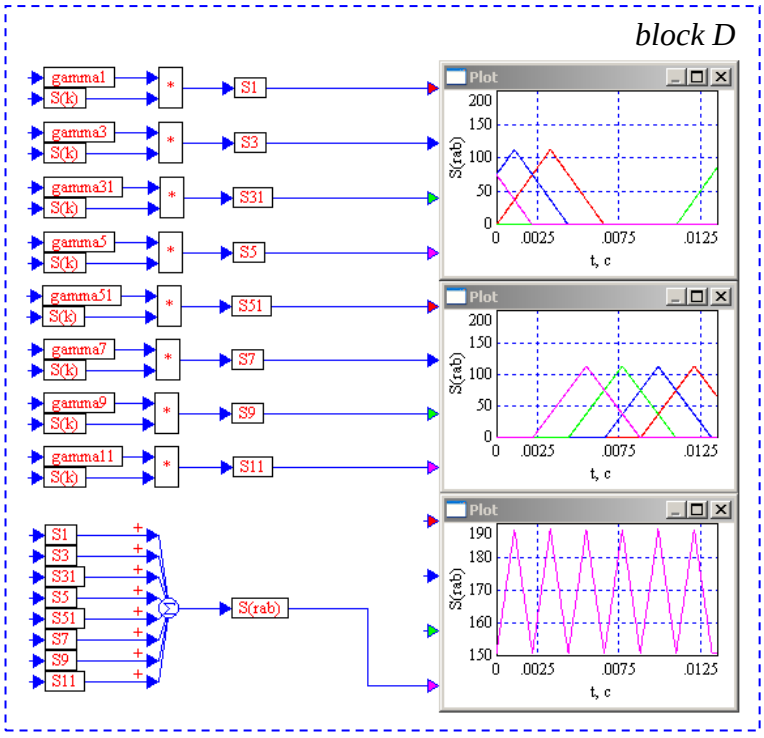


Fig. 5. Dynamic model block for determining the variation in the overlap area of the ports of the movable and stationary distributors

Block **F** (Fig. 6) allows the variation in the working fluid flow rate through the hydraulic motor, depending on the design features of the distribution system, to be determined using the following expression [5]:

$$Q_{hm}(t)=\mu\cdot\sum_{i=1}^{Z}\left[\left(\frac{\pi}{z_2}-\Delta\right)-\left|\beta_i-\alpha_i(t)\right|\right]\cdot\frac{\left(R_2^2-R_1^2\right)}{2}\cdot\sqrt{\frac{2p(t)}{\rho}}. \quad (7)$$

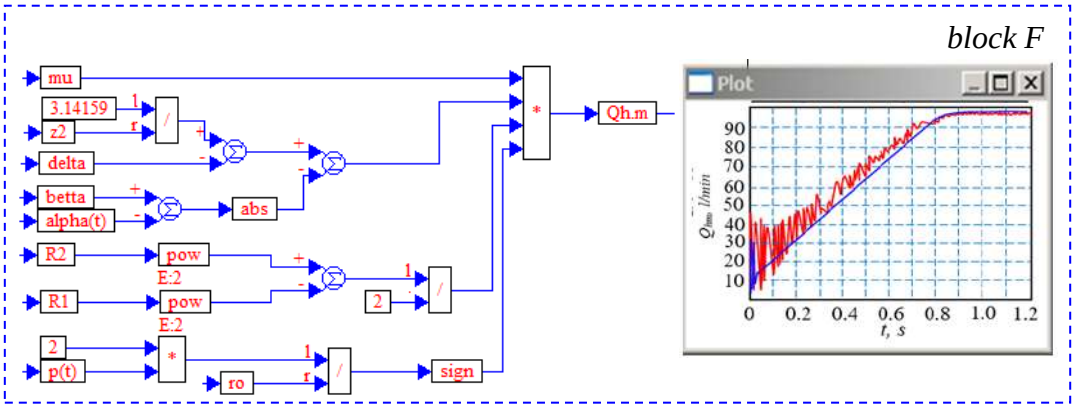


Fig. 6. Dynamic model block for determining the variation in the working fluid flow rate through the hydraulic motor

Block **G** (Fig. 7) allows the variation in the working fluid flow rate through the relief valve to be determined using the following expression [1]:

$$Q_{val}(t) = \mu \cdot \pi \cdot d_{pl} \cdot x(t) \cdot \sqrt{\frac{2p_1(t)}{\rho}}. \quad (8)$$

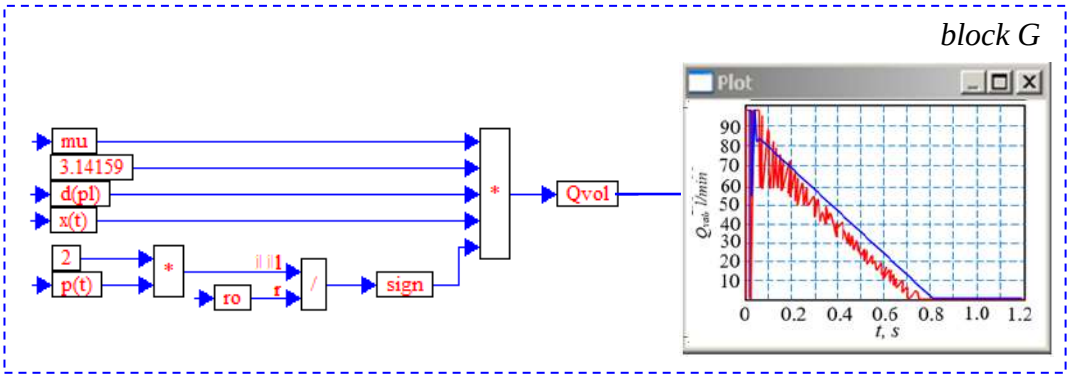


Fig. 7. Dynamic model block for determining the variation in the working fluid flow rate through the relief valve

Block **H** (Fig. 8) allows the total angle encompassing the high-pressure zone to be determined using the following expression:

$$\varphi_{high_i}(t) = 2\Delta\varphi_i(t) + \gamma_i(t) \text{ or } \varphi_{high_i}(t) = 2\varepsilon - \gamma_i(t). \quad (9)$$

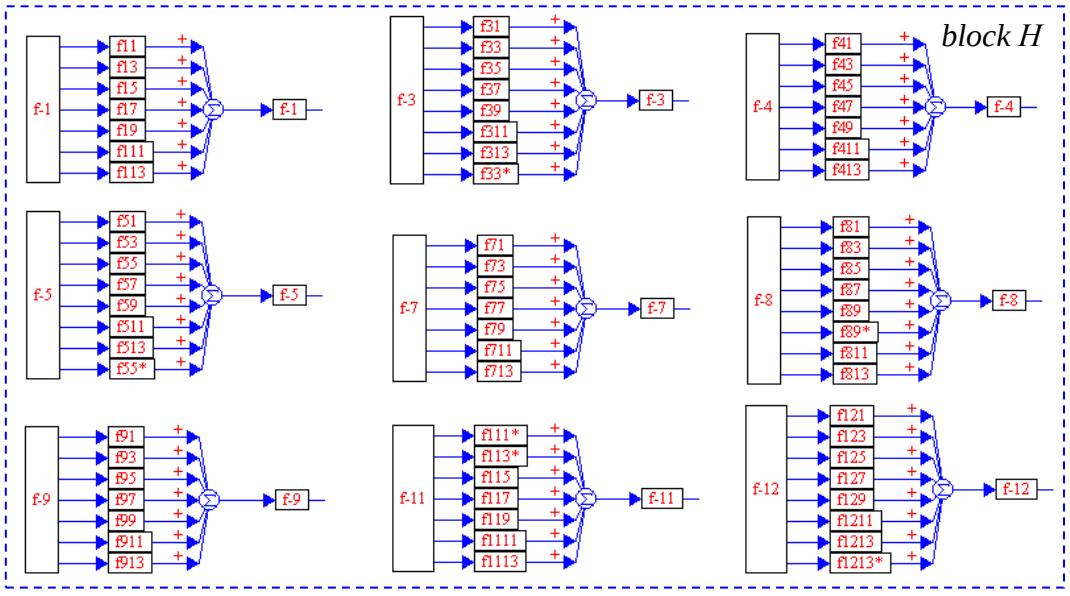


Fig. 8. Dynamic model block for determining the total angle encompassing the high-pressure zone

Block **K** (Fig. 9) allows the variation in volumetric losses in the end-face distribution system at any instant to be determined using the following expression [5]:

$$Q_{hm_{leak}} = \frac{h^3}{12\mu}\sum\varphi_i \cdot \left[p_1(t)\cdot a - \frac{3\rho\cdot\omega_{hm}^2}{20}\cdot b\right], \quad (10)$$

$$a = \frac{\left(\ln\frac{R_1}{R_1^0} - \ln\frac{R_2^0}{R_2}\right)}{\ln\frac{R_1}{R_1^0}\cdot\ln\frac{R_2^0}{R_2}}, \quad b = \frac{\left(R_1^{02} - R_1^2\right)}{\ln\frac{R_1}{R_1^0}} + \frac{\left(R_2^2 - R_2^{02}\right)}{\ln\frac{R_2^0}{R_2'}},$$

where h is the gap height between the contacting surfaces of the movable and stationary distributors; p_1 is the pressure in the hydraulic drive of the mechatronic system; R_1 and R_2 are the inner and outer radii of the movable and stationary distributors, $R_1 = R_1^0 - b_1$, $R_2 = R_2^0 - b_2$.

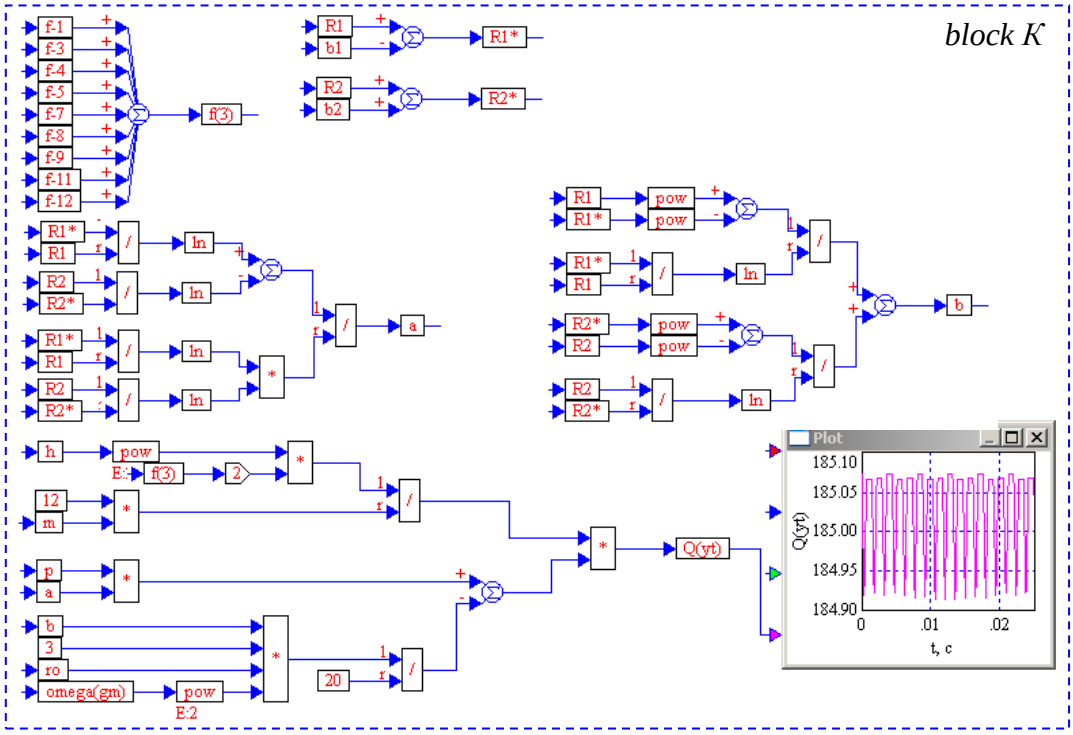


Fig. 9. Dynamic model block for determining the variation in volumetric losses in the end-face distribution system at any instant

Block **L** (Fig. 10) allows the variation in torque on the shafts of the standard and modernized hydraulic motors to be determined using the following expression [9]:

$$M_{tor}(t) = 2\left(e \pm \frac{G}{2}\right) \cdot p_1(t) \cdot b \cdot (z_1 + 1) \cdot h_i. \tag{11}$$

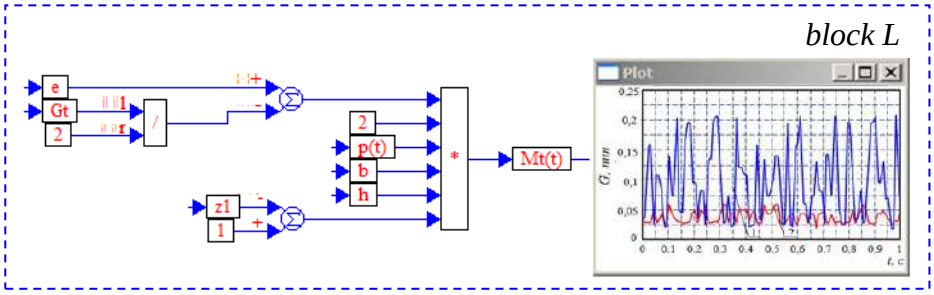


Fig. 10. Dynamic model block for determining the variation in torque on the hydraulic motor shaft at any instant

Block **M** (Fig. 11) includes the calculation of pressure variation and its subsequent correction to account for changes in the flow area of the distribution system. The basic equation for pressure variation without a passive pulsation damper is given by [30]:

$$\frac{dp_1(t)}{dt} = \frac{2 \cdot E_{fl}}{\left(V_{p0} + V_{hm0}\right)} \cdot \left[\frac{V_{p0}}{2\pi} \cdot \omega_p(t) \cdot e - \frac{V_{hm0}}{2\pi} \cdot \omega_{hm}(t) - C_{p.leak} \cdot \left[p_1(t) - p_{dr}\right] - \right.$$
$$\left. - C_{p.fl} \cdot \left[p_1(t) - p_{suc}\right] - C_{hm.fl} \cdot p_1(t) - C_{hm.fl} \cdot \left[p_1(t) - p_{dr}\right] - \frac{1}{E_{fl}} \times \right. \tag{12}$$

$$\times\left[C_p\cdot\omega_p(t)+C_{hn}\cdot\omega_{hm}(t)\right]\cdot\left[p_1(t)-p_{dr}\right]-Q_{vol}(t)\Big]$$

The factor $2E_{fl}/(V_{p0}+V_{hm0})$ in equation (12) corresponds to the representation adopted in [30] for the flow rate components associated with pressure changes in the pump and hydraulic motor, with the coefficients $V_{p0}/(2E_{fl})$ and $V_{hm0}/(2E_{fl})$, respectively.

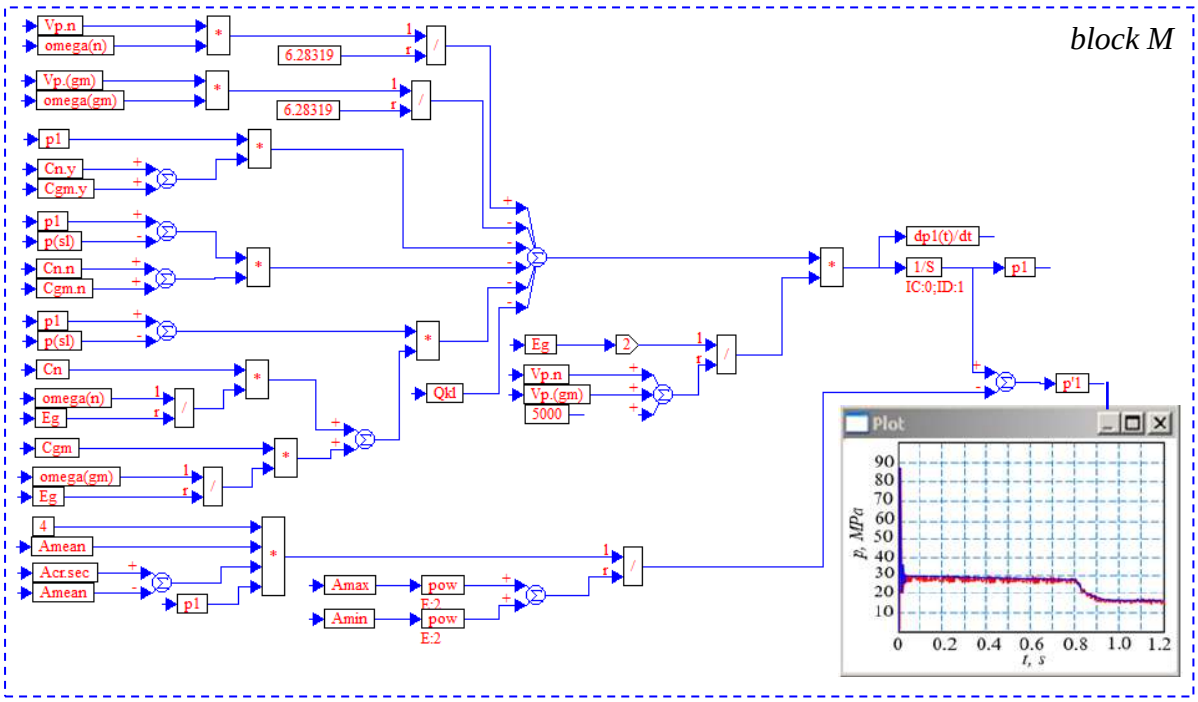


Fig. 11. Dynamic model block for determining the pressure variation in the hydraulic drive at any instant

The pressure $p_1(t)$ is determined by integrating equation (12). In block **M** (Fig. 11), the effect of changes in the flow area of the distribution system is taken into account by applying a separate algebraic correction to the calculated pressure:

$$p_{1,corr}(t)=p_1(t)-\frac{4A_{mean}\left[A_{cr.sec}(t)-A_{mean}\right]p_1(t)}{A^2_{\max}(t)+A^2_{min}(t)}. \qquad (13)$$

where $p_{1,\mathrm{corr}(t)}$ is the pressure with this correction applied, denoted by p'_1 in Fig. 11.

Figure 11 shows the configuration of block **M** with a passive pulsation damper of volume V_{ppd} = 5000 cm³, used to obtain the results presented in Figs. 23–27. In this implementation, the coefficient multiplying the resultant flow rate in the pressure variation equation is taken as $2E_{fl}/(V_{p0}+V_{hm0}+V_{ppd})$. When $V_{ppd}=0$, this coefficient corresponds to the basic equation (12).

Block **N** (Fig. 12) allows uneven pump delivery $Q_p(t)$ and changes in the load on the active working element, characterized by the resisting torque $M_r(t)$, to be specified. External disturbances were considered in studies [8, 30]. Taking into account the structure of block **N** (Fig. 12), these inputs are represented as follows:

$$\begin{cases} Q_p(t)=Q_{p,0}+\Delta Q_p(t). \\ M_c(t)=\max\left\{0, M_{кр}(t)\left[1-\exp\left(-\dfrac{r(t)}{T}\right)\right]+M_\omega\cdot\sin(\omega_M t)\right\}. \end{cases} \qquad (14)$$

where $Q_{p,0}$ is the constant component of pump delivery; $\Delta Q_p(t)$ is the variable component of pump delivery generated by the signal generators and switching blocks in block **N** (Fig. 12). In the expression for the resisting torque, $r(t)$ is the signal from the ramp generator shown in Fig. 12; T is the time constant of the exponential rise; $M_{tor}(t)$ is the torque input signal denoted

by $M_t(t)$ in the diagram; M_ω and ω_M are the amplitude and angular frequency of the harmonic torque component. The operation max{0, …} corresponds to replacing negative values of the resultant signal with zero in block **N**.

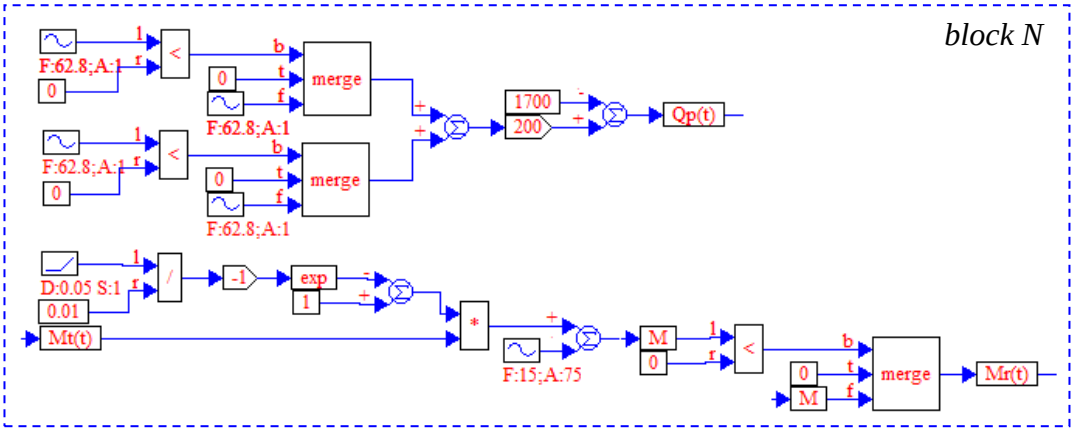


Fig. 12. Dynamic model block for specifying uneven pump delivery and changes in the load on the active working element at any instant

The presented structural and functional blocks (Figs. 2–12) explain the modeling of transient processes in the hydraulic drive of the mechatronic system, taking into account the design features of the rotor system and distribution system of the planetary hydraulic motor, external disturbances, and passive damping. The results are considered below for individual computational cases, with the initial conditions and sources of previously obtained data specified.

Results.

At the beginning of acceleration of the hydraulic drive of the mechatronic system, a brief start-up pressure surge is observed. According to the curves in Fig. 13, the maximum pressure is approximately 88 MPa for the standard hydraulic motor (curve 1) and 85 MPa for the modernized hydraulic motor (curve 2). After the start-up surge, the pressure drops sharply. Subsequently, for the standard hydraulic motor, the pressure level gradually decreases from 29 to 26.5 MPa, with oscillations having an amplitude of approximately 2–2.5 MPa (Fig. 13, curve 1).

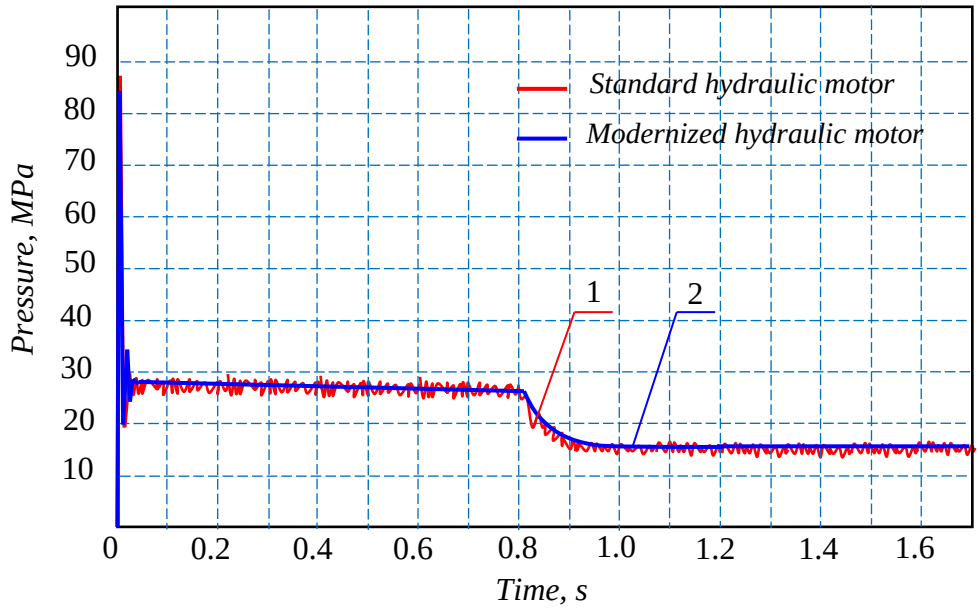


Fig. 13. Pressure variation during acceleration of the hydraulic drive of the mechatronic system: 1 – standard hydraulic motor; 2 – modernized hydraulic motor

The pressure oscillations during the period t = 0.007–0.8 s are associated with changes in the flow area of the distribution system of the standard hydraulic motor. During further acceleration (t = 0.8–0.9 s), the pressure decreases to the value corresponding to steady-state operation. At t > 0.9 s, the amplitude of the pressure oscillations is approximately 1.5 MPa. In the computational case considered, no pressure oscillations caused by changes in the flow area of the distribution system are observed for the modernized hydraulic motor, since this area remains constant (Fig. 13, curve 2).

During acceleration of the hydraulic drive with the standard hydraulic motor, significant pulsations in the working fluid flow rate through the hydraulic motor are observed in the initial stage of the transient process (t = 0–0.08 s) (Fig. 14, curve 1). According to [7], their magnitude reaches 40 L/min. Subsequently, during the period t = 0.08–0.9 s, the flow rate gradually increases, while the pulsations decrease. At t > 0.9 s, the flow rate reaches its steady-state value with small pulsations, whose magnitude, according to [7], is up to 2 L/min. In the computational case considered, no flow rate oscillations caused by changes in the flow area of the distribution system are observed for the modernized hydraulic motor, since this area remains constant (Fig. 14, curve 2).

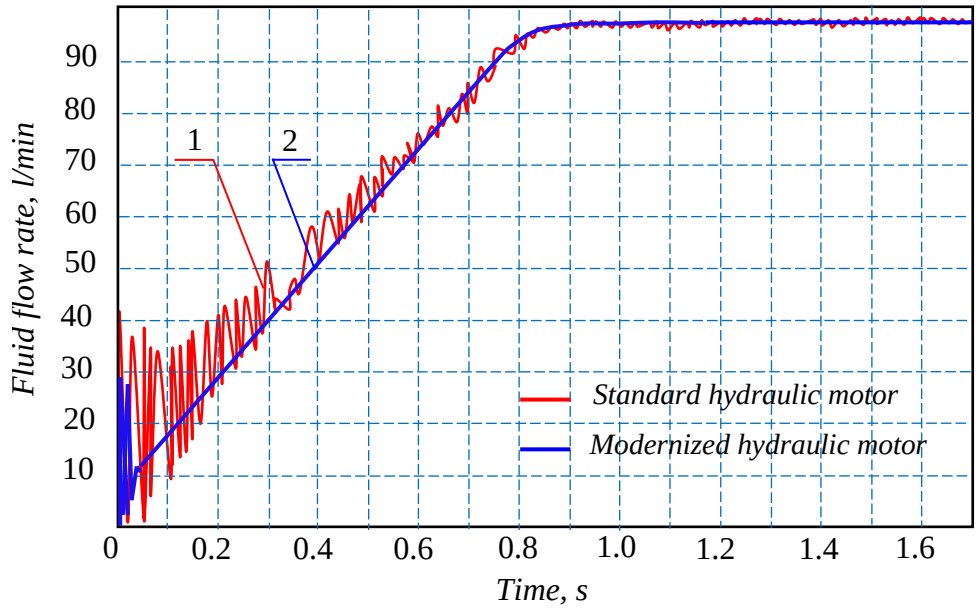


Fig. 14. Variation in the working fluid flow rate through the hydraulic motor during acceleration of the hydraulic drive of the mechatronic system: 1 – standard hydraulic motor; 2 – modernized hydraulic motor

In the initial stage of acceleration of the hydraulic drive with the standard hydraulic motor (t = 0–0.08 s), the working fluid flow rate through the relief valve reaches a maximum value of approximately 98 L/min and exhibits significant pulsations, whose magnitude, according to [7], is up to 40 L/min. These pulsations are associated with changes in the flow area of the distribution system of the standard hydraulic motor (Fig. 15, curve 1).

As acceleration proceeds, the working fluid flow rate through the relief valve gradually decreases. For the standard hydraulic motor, the magnitude of the flow rate pulsations also decreases. According to the curves in Fig. 15, flow through the valve ceases at approximately t = 0.85 s for the standard hydraulic motor (curve 1) and t = 0.75 s for the modernized hydraulic motor (curve 2), corresponding to valve closure. In the computational case considered, no oscillations in the flow rate through the valve caused by changes in the flow area of the distribution system are observed for the modernized hydraulic motor.

During start-up of the hydraulic drive (t = 0–0.02 s), a brief torque peak is observed on the hydraulic motor shaft, reaching approximately 2000 N·m for both designs considered (Fig. 16). Subsequently, during the interval t = 0.04–0.8 s for the standard hydraulic motor

and t = 0.04–0.72 s for the modernized hydraulic motor, the torque level gradually decreases from 630 to 620 N·m. According to [2], changes in the diametral clearance in the rotor system of the standard hydraulic motor are accompanied by torque oscillations with an amplitude of up to 120–130 N·m (Fig. 16, curve 1).

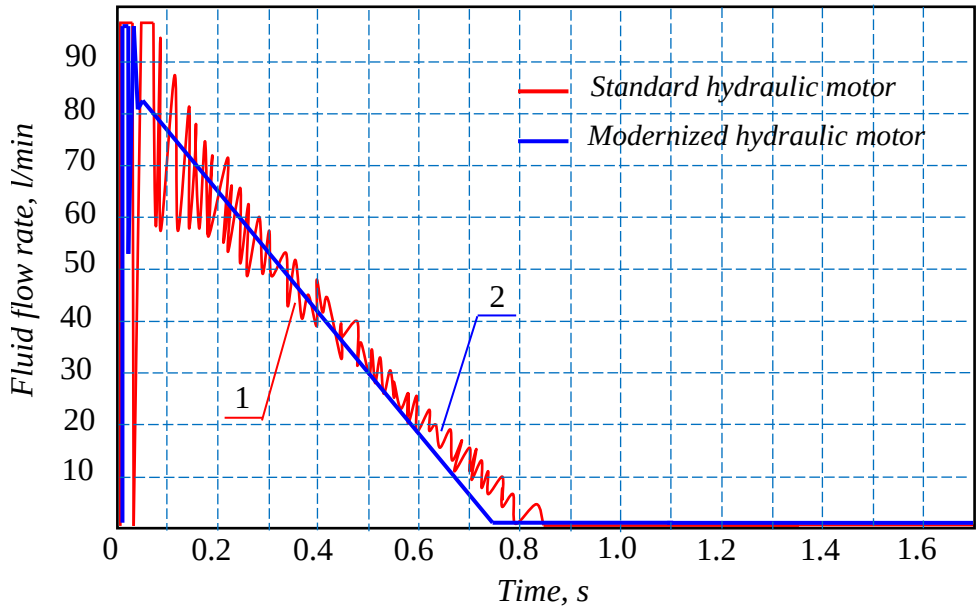


Fig. 15. Variation in the working fluid flow rate through the relief valve during acceleration of the hydraulic drive of the mechatronic system: 1 – standard hydraulic motor; 2 – modernized hydraulic motor

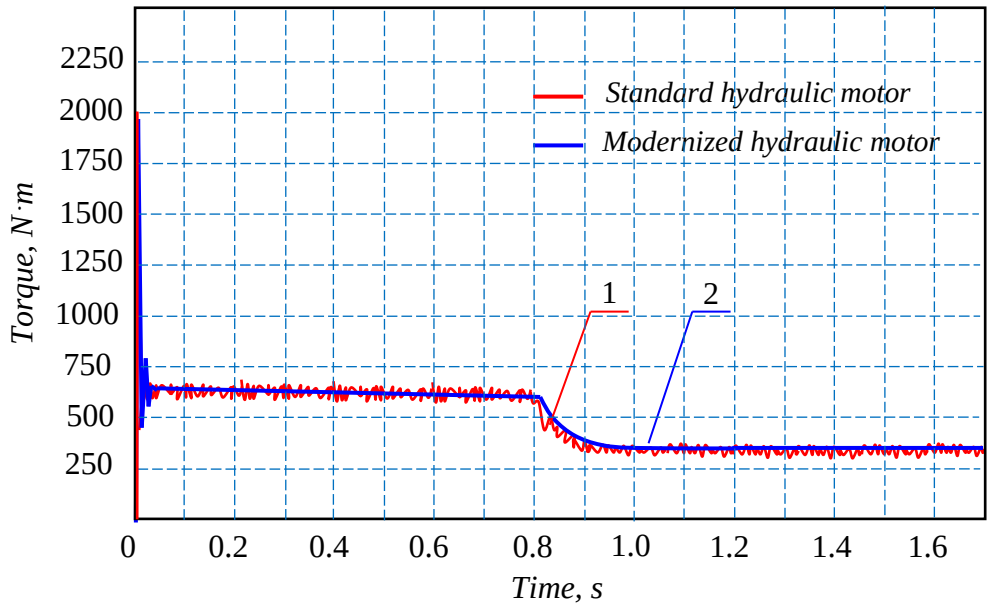


Fig. 16. Torque variation during acceleration of the hydraulic drive of the mechatronic system: 1 – standard hydraulic motor; 2 – modernized hydraulic motor

During further acceleration, the torque decreases to its steady-state level during the interval t = 0.8–0.9 s for the standard hydraulic motor and t = 0.72–0.8 s for the modernized hydraulic motor [2]. At t > 0.9 s, the transient process is practically complete for both designs. However, torque oscillations persist in the standard hydraulic motor, with an amplitude of up to 63 N·m according to [2] (Fig. 16, curve 1). For the modernized hydraulic motor, no pronounced torque pulsations are observed in the curve for the computational case considered (Fig. 16, curve 2).

During acceleration of the hydraulic drive, the shaft rotational speed of the standard and modernized hydraulic motors gradually increases to a steady-state value of approximately 600 min^{-1} (Fig. 17). According to [2], this operating condition is reached at approximately t = 0.9 s for the standard hydraulic motor and t = 0.8 s for the modernized hydraulic motor. Thus, under the conditions considered, both designs provide practically the same steady-state rotational speed, but their acceleration durations differ.

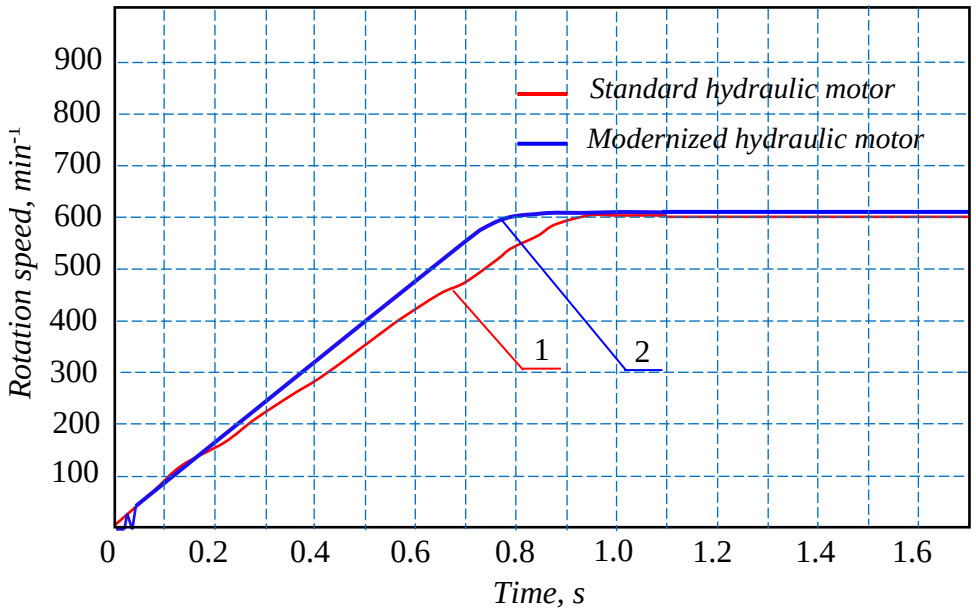


Fig. 17. Variation in the hydraulic motor shaft rotational speed during acceleration of the hydraulic drive of the mechatronic system: 1 – standard hydraulic motor; 2 – modernized hydraulic motor

The results considered [7] show that changes in the flow area of the distribution system of the standard hydraulic motor within the range A_{th} = 222–226 mm² are accompanied by pulsations in pressure and working fluid flow rate. When the flow area of the modernized distribution system remains constant at A_{th} = 226 mm², pulsations caused by changes in this area are not observed.

The results of the rotor system study [2] show that changes in the diametral clearance within the range G = 0.055–0.21 mm are accompanied by torque pulsations in the standard hydraulic motor. For the modernized design, with clearance varying within the range G = 0.05–0.06 mm, no pronounced torque pulsations are observed in the computational case considered. These results characterize the operation of the hydraulic drive at constant pump delivery and resisting torque, without a passive pulsation damper.

The results of the study of the dynamic characteristics of the hydraulic drive under variable external inputs, presented in [8], are considered below. Operating conditions were simulated by uneven pump delivery and changes in the resisting torque on the active working element. In study [8], the clearance between the rotors of the standard hydraulic motor varied within the range G = 0.02–0.21 mm, and the flow area of the distribution system varied within the range A_{th} = 200–226 mm². For the modernized hydraulic motor, the corresponding parameters were G = 0.02–0.065 mm and A_{th} = 226 mm². Thus, the geometric parameters of this computational case differ from those of studies [2, 7] considered above.

In the initial period of acceleration of the hydraulic drive (t = 0–0.02 s), a brief pressure surge is observed, reaching approximately 90 MPa for the standard hydraulic motor and 85 MPa for the modernized hydraulic motor [8] (Fig. 18). After the start-up surge, the pressure drops sharply, and its level then gradually decreases from approximately 29 to 27 MPa. During this stage, pressure pulsations associated with changes in the flow area of the distribution system and uneven pump delivery are observed for the standard hydraulic motor.

For the modernized hydraulic motor, the pulsations during this stage are much less pronounced.

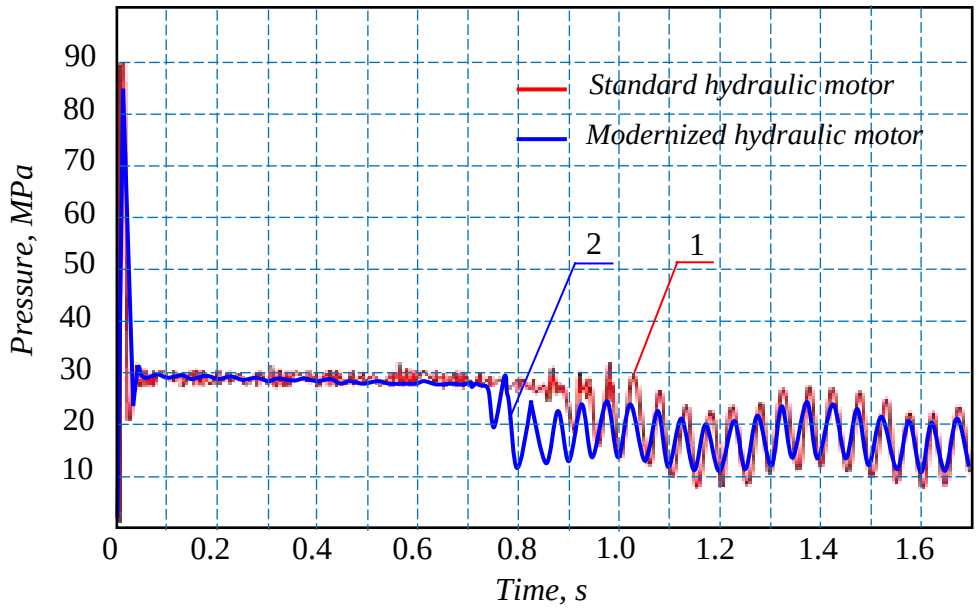


Fig. 18. Pressure variation during acceleration of the hydraulic drive of the mechatronic system during operation of self-propelled machinery: 1 – standard hydraulic motor; 2 – modernized hydraulic motor

During the subsequent stage of the transient process, the mean pressure level decreases, but pronounced oscillations caused by variable external inputs persist. According to the curves in Fig. 18, the peak-to-peak magnitude of these oscillations is smaller for the modernized hydraulic motor than for the standard hydraulic motor. Thus, modernization reduces pressure oscillations in the operating mode considered but does not eliminate them completely.

During acceleration of the hydraulic drive, the overall level of the working fluid flow rate through the hydraulic motor gradually increases (Fig. 19). For the standard hydraulic motor, this process is accompanied by pronounced pulsations associated with changes in the flow area of the distribution system and uneven pump delivery (curve 1). For the modernized hydraulic motor, the flow rate varies more smoothly, but the oscillations do not disappear completely (curve 2).

After the main acceleration stage, the flow rate oscillates around a steady mean level. According to [8], the magnitude of the pulsations during this stage is up to 3 L/min for the standard hydraulic motor and up to 2 L/min for the modernized hydraulic motor. The remaining pulsations are associated with uneven pump delivery.

During the initial start-up period of the hydraulic drive, the working fluid flow rate through the relief valve reaches approximately 98 L/min for both hydraulic motor designs considered [8]. As acceleration proceeds, the overall flow rate level decreases, while pronounced pulsations persist (Fig. 20). The flow rate oscillations are larger for the standard hydraulic motor than for the modernized hydraulic motor.

During the final stage of valve operation, the flow rate periodically drops to zero, after which individual flow pulses occur again. According to the curves in Fig. 20, flow finally ceases at approximately t = 0.95 s for the standard hydraulic motor (curve 1) and t = 0.75 s for the modernized hydraulic motor (curve 2). These values characterize the cessation of flow through the relief valve in the computational case considered.

During the initial start-up period of the hydraulic drive (t = 0–0.02 s), a brief torque surge is observed, reaching approximately 2100 N·m for the standard hydraulic motor and 1900 N·m for the modernized hydraulic motor [8] (Fig. 21). After the start-up surge, the torque

level decreases to 640–620 N·m. During this stage, pronounced pulsations associated with the design features of the rotor system are observed for the standard hydraulic motor (curve 1). For the modernized hydraulic motor, the torque varies more smoothly (curve 2).

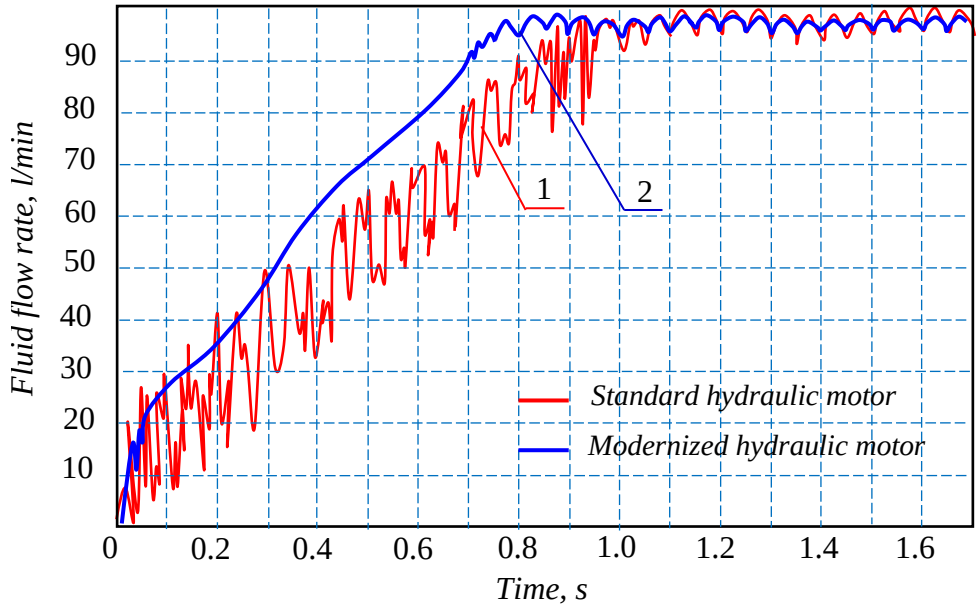


Fig. 19. Variation in the working fluid flow rate through the hydraulic motor during acceleration of the hydraulic drive of the mechatronic system during operation of self-propelled machinery: 1 – standard hydraulic motor; 2 – modernized hydraulic motor

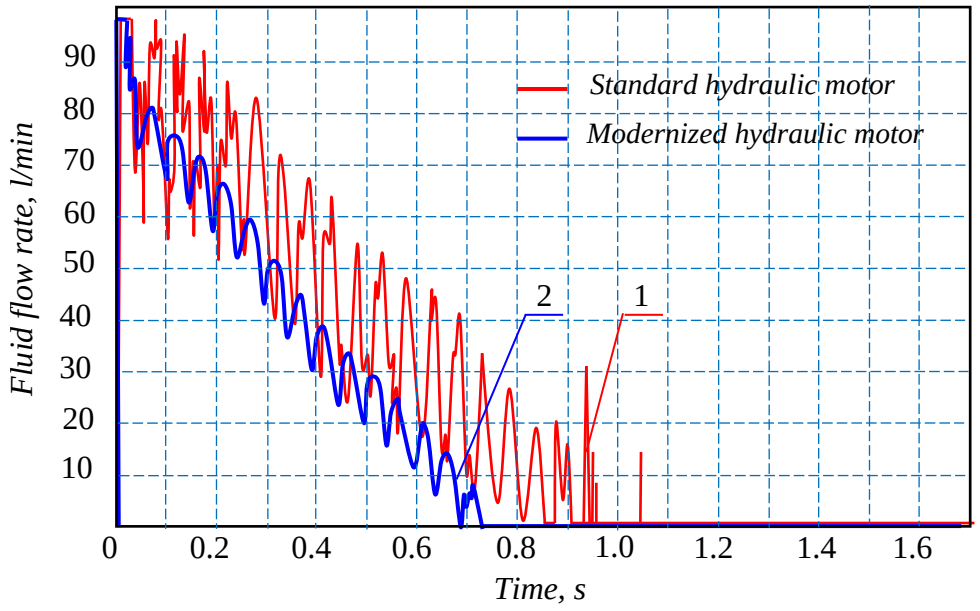


Fig. 20. Variation in the working fluid flow rate through the relief valve during acceleration of the hydraulic drive of the mechatronic system during operation of self-propelled machinery: 1 – standard hydraulic motor; 2 – modernized hydraulic motor

During the subsequent stage of the transient process, the mean torque level decreases. However, oscillations associated with changes in the resisting torque persist for both designs. According to the curves in Fig. 21, the peak-to-peak magnitude of these oscillations is smaller for the modernized hydraulic motor than for the standard hydraulic motor. Thus, in the operating mode considered, modernization reduces torque oscillations but does not eliminate them completely.

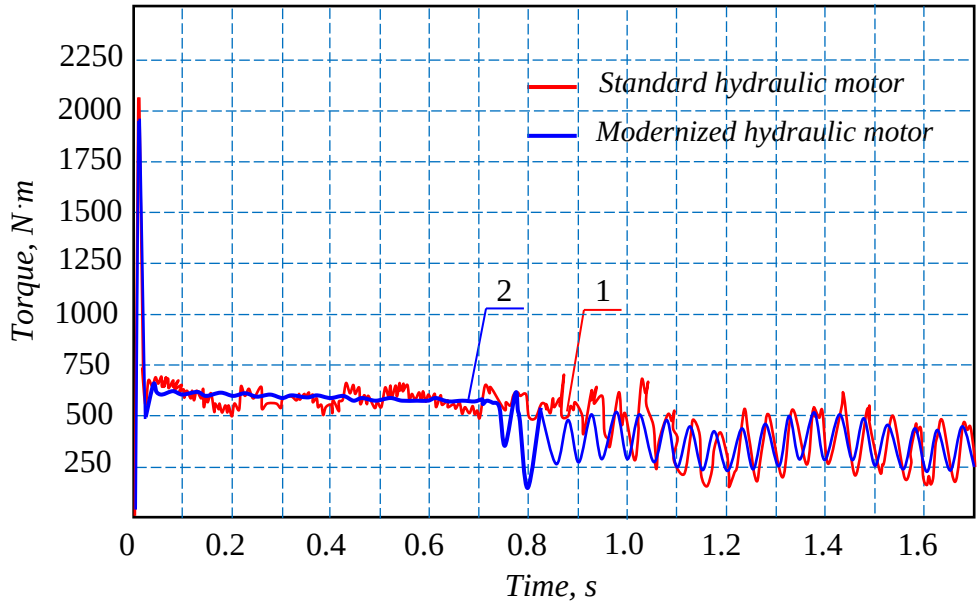


Fig. 21. Torque variation during acceleration of the hydraulic drive of the mechatronic system during operation of self-propelled machinery: 1 – standard hydraulic motor; 2 – modernized hydraulic motor

During acceleration of the hydraulic drive, the shaft rotational speed of the standard and modernized hydraulic motors increases, approaching a mean level of approximately 600 min^{-1} (Fig. 22). The modernized hydraulic motor reaches this level earlier than the standard hydraulic motor. After the main acceleration stage, the rotational speed of both designs continues to oscillate around the mean value due to uneven pump delivery and changes in the resisting torque [8].

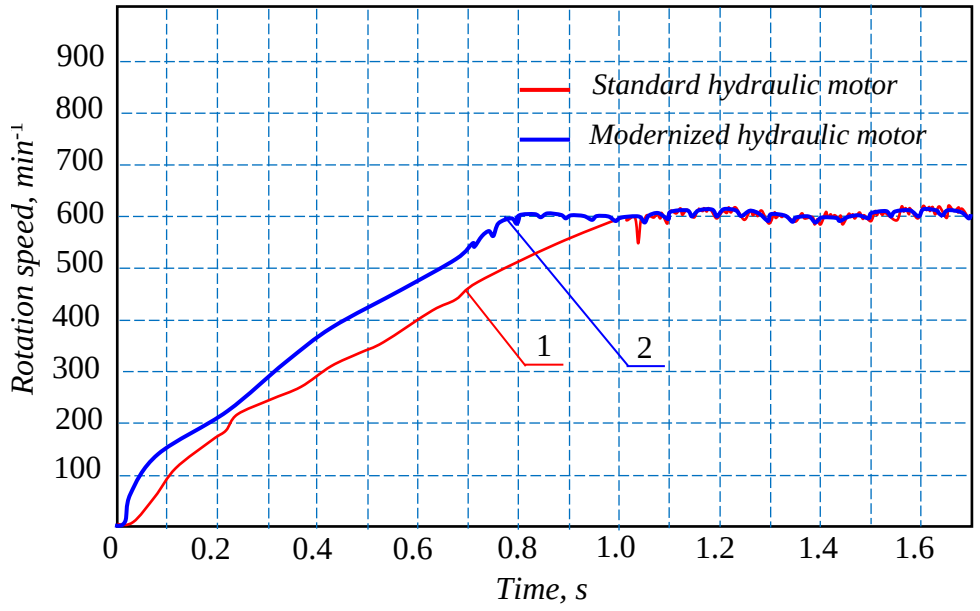


Fig. 22. Variation in the hydraulic motor shaft rotational speed during acceleration of the hydraulic drive of the mechatronic system during operation of self-propelled machinery: 1 – standard hydraulic motor; 2 – modernized hydraulic motor

The results considered [8] show that, under variable external inputs, the modernized hydraulic motor reaches the operating rotational speed level more quickly and exhibits smaller pressure and torque oscillations than the standard hydraulic motor. These differences are associated with a reduction in the clearance between the rotor teeth and the elimination of

changes in the flow area of the distribution system. However, modernization does not eliminate oscillations in the output characteristics caused by uneven pump delivery and changes in the load.

The third computational case considers the operation of the hydraulic drive with a passive pulsation damper of 5000 cm³ under variable external inputs. The use of such a damper to reduce dynamic loads is considered in [14]. Figures 23–27 present the simulation results for the corresponding processes in the standard and modernized hydraulic motors, obtained by the authors using the VisSim package.

During start-up of the hydraulic drive with a passive pulsation damper, a brief increase in pressure is observed. According to the curves in Fig. 23, the peak pressure is approximately 38 MPa for the standard hydraulic motor (curve 1) and 36 MPa for the modernized hydraulic motor (curve 2). These values are lower than the start-up maxima shown in Fig. 18 for the hydraulic drive without a damper. After the start-up surge, the pressure drops to approximately 29 MPa and then gradually decreases. During acceleration, the pressure oscillations are more pronounced for the standard hydraulic motor than for the modernized hydraulic motor.

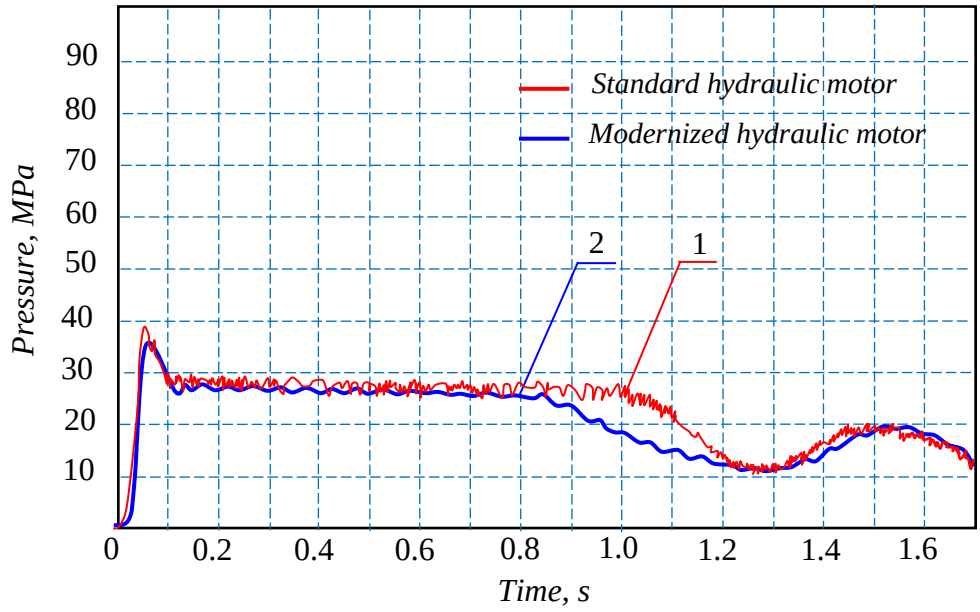


Fig. 23. Pressure variation during acceleration of the hydraulic drive of the mechatronic system during operation of self-propelled machinery with a passive pulsation damper: 1 – standard hydraulic motor; 2 – modernized hydraulic motor

As the mean pressure level decreases further, smooth oscillations associated with changes in the resisting torque persist for both designs. Thus, in the computational case presented, the use of a passive damper is accompanied by a reduction in start-up pressure peaks but does not completely eliminate oscillations under variable load.

The curves in Fig. 24 show the variation in the working fluid flow rate through the hydraulic motor when a passive pulsation damper is used. During acceleration, the mean flow rate increases, approaching 100 L/min. For the standard hydraulic motor (curve 1), this increase is accompanied by pronounced pulsations. For the modernized hydraulic motor (curve 2), the flow rate increases more smoothly and reaches the level corresponding to the end of the main acceleration stage earlier.

After acceleration, flow rate oscillations persist for both designs, with more pronounced oscillations in the standard hydraulic motor. Thus, in the hydraulic drive with a passive pulsation damper considered here, the modernized hydraulic motor exhibits smoother flow rate variation both during acceleration and during subsequent operation under variable external inputs.

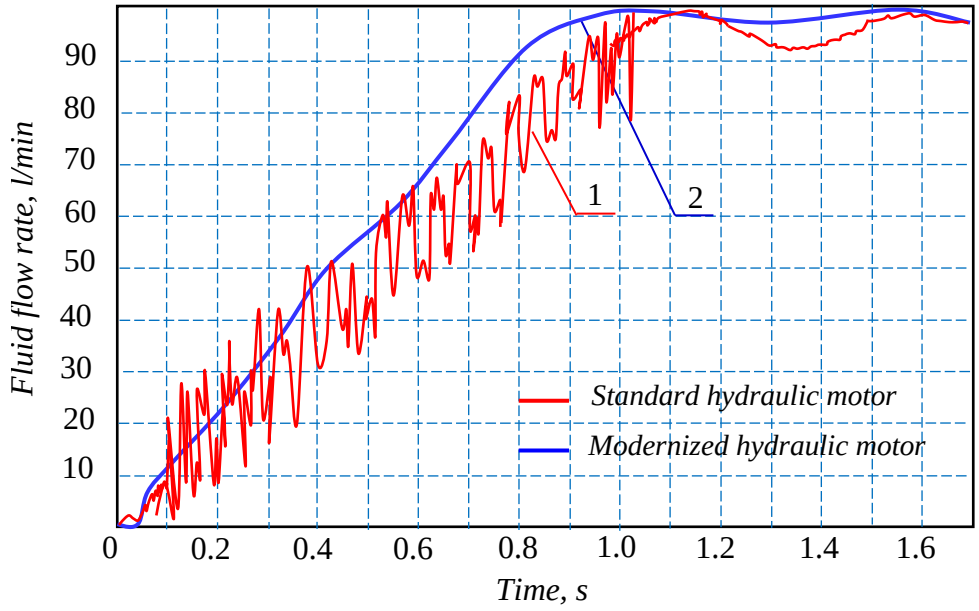


Fig. 24. Variation in the working fluid flow rate through the hydraulic motor during acceleration of the hydraulic drive of the mechatronic system during operation of self-propelled machinery with a passive pulsation damper: 1 – standard hydraulic motor; 2 – modernized hydraulic motor

Figure 25 presents the curves of the working fluid flow rate through the relief valve when a passive pulsation damper is used. At the beginning of start-up, there is no flow through the valve. The flow rate then briefly rises to a maximum value of approximately 98 L/min. Subsequently, as the hydraulic motor accelerates, the mean flow rate through the valve decreases. This process is accompanied by pulsations that are more pronounced for the standard hydraulic motor (curve 1) than for the modernized hydraulic motor (curve 2).

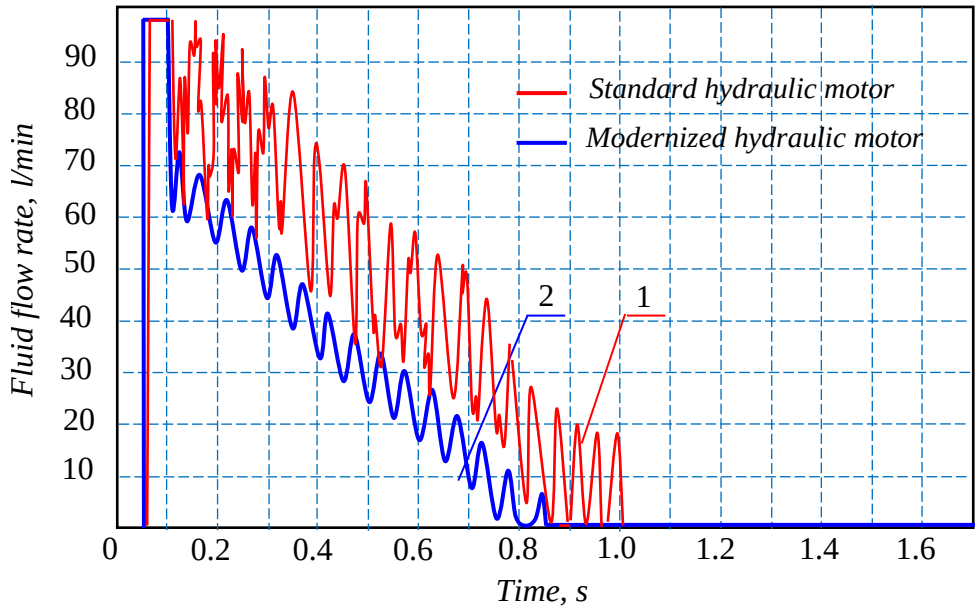


Fig. 25. Variation in the working fluid flow rate through the relief valve during acceleration of the hydraulic drive of the mechatronic system during operation of self-propelled machinery with a passive pulsation damper: 1 – standard hydraulic motor; 2 – modernized hydraulic motor

According to the curves, flow through the relief valve ceases after the final pulsations at approximately t = 1.0 s for the standard hydraulic motor and t = 0.85 s for the modernized

hydraulic motor. During the subsequent period shown in the curves, the flow rate through the valve remains zero.

During start-up of the hydraulic drive with a passive pulsation damper, a brief torque surge is observed (Fig. 26). According to the curves presented, the peak values for both designs are approximately within the range of 900–1000 N·m. After the start-up surge, the torque decreases to approximately 600–650 N·m, and its mean value then gradually decreases. During this stage, torque oscillations are more pronounced for the standard hydraulic motor (curve 1) than for the modernizsed hydraulic motor (curve 2).

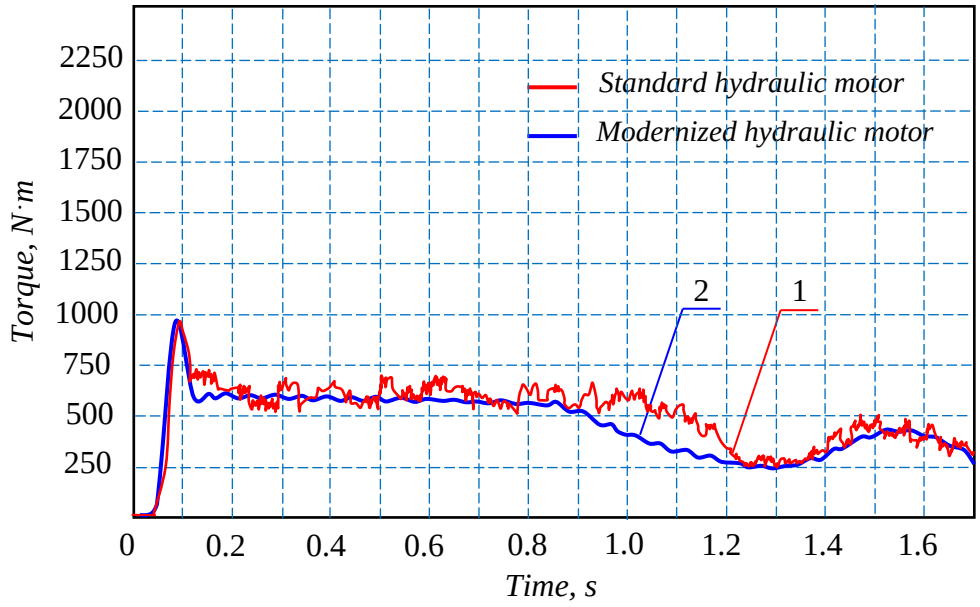


Fig. 26. Torque variation during acceleration of the hydraulic drive of the mechatronic system during operation of self-propelled machinery with a passive pulsation damper: 1 – standard hydraulic motor; 2 – modernized hydraulic motor

The subsequent decrease in the mean torque level begins earlier for the modernized hydraulic motor than for the standard hydraulic motor. During further operation, smooth torque oscillations persist for both designs under variable external load. A comparison of Figs. 21 and 26 shows that, in the computational case presented with a passive pulsation damper, the start-up torque maxima are substantially lower than in the case without a damper. However, torque oscillations are not completely eliminated.

Figure 27 presents the variation in the hydraulic motor shaft rotational speed when a passive pulsation damper is used. During acceleration, the rotational speed of both designs increases, approaching approximately 600 min^{-1}. The modernized hydraulic motor (curve 2) reaches this level earlier than the standard hydraulic motor (curve 1).

After the main acceleration stage, the rotational speed oscillates around the mean level reached. Under the variable external inputs considered, these oscillations are more pronounced for the standard hydraulic motor than for the modernized hydraulic motor. Thus, the use of a passive pulsation damper does not eliminate rotational speed oscillations during subsequent operation of the hydraulic drive.

A comparison of the computational cases considered without a damper and with a passive pulsation damper of 5000 cm^3 shows a reduction in start-up pressure and torque maxima when the damper is used. In Fig. 18, the peak pressure values are approximately 90 and 85 MPa for the standard and modernized hydraulic motors, respectively, whereas in Fig. 23 they are approximately 38 and 36 MPa. The start-up torque maxima decrease from approximately 2100 and 1900 N·m (Fig. 21) to values within the range of 900–1000 N·m (Fig. 26).

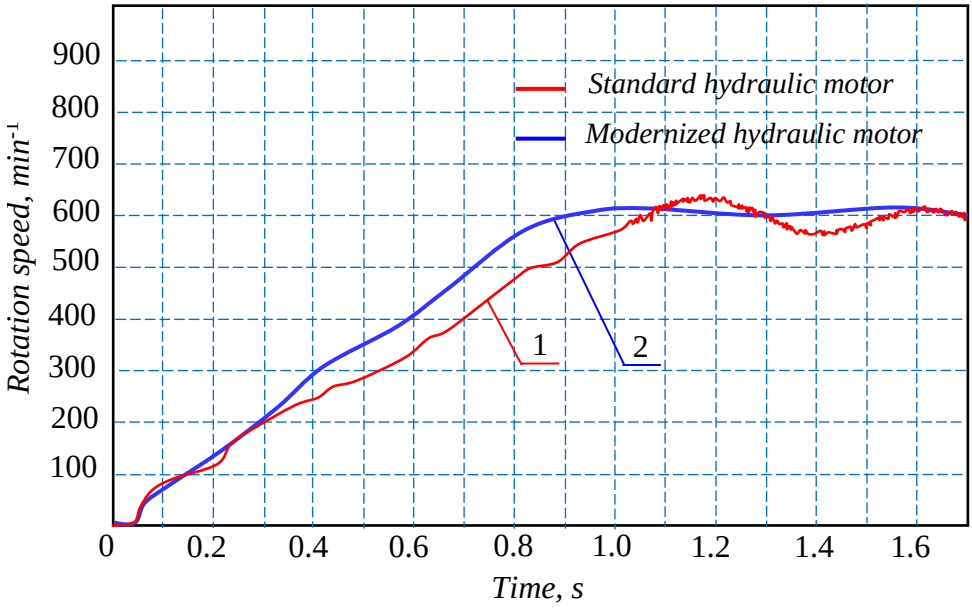


Fig. 27. Variation in the hydraulic motor shaft rotational speed during acceleration of the hydraulic drive of the mechatronic system during operation of self-propelled machinery with a passive pulsation damper: 1 – standard hydraulic motor; 2 – modernized hydraulic motor

Differences between the characteristics of the standard and modernized hydraulic motors persist in the hydraulic drive with a passive pulsation damper. The modernized hydraulic motor exhibits smoother variations in flow rate and torque during acceleration and reaches the operating rotational speed level earlier. However, under variable external inputs, oscillations in the output parameters persist for both designs.

Discussion.

A comparison of the results considered allows discussion of the effects of the design features of the planetary hydraulic motor, variable external inputs, and a passive pulsation damper on the dynamic characteristics of the hydraulic drive. The computational cases presented bring together the results of studies of the rotor and distribution systems [2, 7], hydraulic drive operation under operating disturbances [8], and the use of a passive pulsation damper [14]. When comparing these cases, differences in the initial geometric parameters and calculation conditions must be taken into account. Therefore, differences between individual cases cannot always be explained by a change in only one factor.

At constant pump delivery and resisting torque, changes in the flow area of the distribution system are accompanied by pressure and flow rate pulsations [7], while changes in the diametral clearance between the rotors are accompanied by torque oscillations [2]. For the modernized design with a constant flow area and a smaller range of clearance variation, the corresponding pulsations are less pronounced. These results help identify directions for improving the hydraulic motor design. However, pressure, flow rate, and torque are interrelated, so the effects of the rotor and distribution systems should not be considered completely independent.

Under variable pump delivery and resisting torque, the modernized hydraulic motor also exhibits smoother variations in the output parameters and reaches the operating rotational speed level earlier [8]. However, design modernization does not eliminate oscillations caused by external inputs. Therefore, the reduction of internal sources of pulsations must be considered together with the operating conditions of the hydraulic drive.

In the computational case with a passive pulsation damper of 5000 cm³, the start-up pressure and torque maxima are lower than in the case considered without a damper. However, both the differences between the standard and modernized hydraulic motors and the

oscillations during subsequent operation under variable load persist. This allows the passive damper to be considered an additional means of reducing start-up dynamic loads. The results presented do not justify extending the degree of reduction in start-up maxima to all subsequent oscillations in pressure, flow rate, and torque.

The operation of the relief valve must also be taken into account when interpreting transient processes. The flow rate curves for the valve show individual flow pulses followed by cessation of flow. The time at which flow ceases characterizes valve operation but does not, by itself, determine the completion of hydraulic motor acceleration. The acceleration duration should be assessed from the rotational speed curve using a common criterion for reaching the operating mode.

The synthesis presented is limited to the designs, parameters, and computational operating conditions considered. Numerical estimates obtained directly from the curves are approximate. A quantitative comparison of oscillations requires identical time intervals and a consistent definition of the measure used, either amplitude or full peak-to-peak magnitude. The reduction in oscillations under the operating conditions considered indicates improved dynamic performance but does not replace a separate study of hydraulic drive stability.

The practical significance of the results considered lies in providing a basis for jointly considering the hydraulic motor design, operating disturbances, and passive damping measures when designing the hydraulic drive. Maintaining a constant flow area of the distribution system and reducing the range of clearance variation between the rotors help reduce the associated pulsations, while the use of a passive damper further limits start-up loads. The selection of specific parameters requires consideration of the operating conditions and permissible oscillations in the output characteristics.

Conclusions.

1. The results of computational studies of the dynamic characteristics of the hydraulic drive of a mechatronic system with standard and modernized planetary hydraulic motors have been summarized. Cases with constant pump delivery and resisting torque, variable external inputs, and the use of a passive pulsation damper have been considered. A comparison of these results makes it possible to assess how design and operating factors are reflected in variations in pressure, flow rate, torque, and rotational speed.

2. Under the computational operating conditions considered, changes in the flow area of the distribution system are accompanied by pulsations in pressure and working fluid flow rate, while changes in the diametral clearance between the rotors are accompanied by torque oscillations. A constant flow area and a smaller range of clearance variation in the modernized hydraulic motor contribute to reducing the corresponding pulsations.

3. Under variable pump delivery and resisting torque, the modernized hydraulic motor exhibits smaller pressure and torque oscillations and reaches the operating rotational speed level earlier than the standard hydraulic motor. However, oscillations in the output parameters caused by external inputs persist for both designs.

4. In the computational case considered with a passive pulsation damper of 5000 cm^3, the start-up pressure maxima are approximately 38 and 36 MPa for the standard and modernized hydraulic motors, respectively, compared with approximately 90 and 85 MPa in the case without a damper. The start-up torque maxima are within the range of 900–1000 N·m for both designs, compared with approximately 2100 and 1900 N·m without a damper. These estimates characterize the reduction in start-up loads under the conditions considered; subsequent oscillations under variable load are not completely eliminated.

5. The results considered support the joint consideration of hydraulic motor design parameters, operating disturbances, and passive damping measures when designing the hydraulic drive. Modernization of the rotor and distribution systems reduces pulsations associated with their geometry, while a passive damper further limits start-up loads. The

quantitative results relate to the computational cases presented and should be applied with due consideration of differences in the initial parameters and operating conditions.

References

1. Panchenko A., Voloshina A., Kiurchev S., Titova O., Onopreychuk D., Stefanov V., Safoniuk I., Pashchenko V., Radionov H., Golubok M. Development of the universal model of mechatronic system with a hydraulic drive. *Eastern-European Journal of Enterprise Technologies*. 2018. 4 (7(94)). 51–60. https://doi.org/10.15587/1729-4061.2018.139577
2. Panchenko A., Voloshina A., Titova O., Panchenko I., Zasiadko A. The Study of Dynamic Processes of Mechatronic Systems with Planetary Hydraulic Motors. *InterPartner 2020: Advanced Manufacturing Processes II*. LNME. Springer, Cham, 2021. 704–713. https://doi.org/10.1007/978-3-030-68014-5_68
3. Kyurchev V., Kiurchev S., Rezvaya K., Pastushenko A., Głowacki S. Experimental Evaluation of the Impact of the Diametral Clearance on Output Characteristics of a Planetary Hydraulic Motor. *DSMIE 2023: Advances in Design, Simulation and Manufacturing VI*. LNME. Springer, Cham, 2023. 84–94. https://doi.org/10.1007/978-3-031-32774-2_9
4. Kiurchev S., Luzan P., Zasiadko A., Radionov H., Boltianska N. Influence of the flow area of distribution systems on changing the operating parameters of planetary hydraulic motors. *IOP Conference Series: Materials Science and Engineering*, 2021. 1021. 012037. https://doi.org/10.1088/1757-899X/1021/1/012037
5. Hutsol T. European Green Deal: Improving the Efficiency of Using Planetary Hydraulic Machines. *Energies*, 2023. 16 (18). 6481. https://doi.org/10.3390/en16186481.
6. Yeremenko, O., Abdullo, M. A., Boltianska, N., Mikhalchenko, S., Verkholantseva, V. Reducing the Pulsation of the Working Fluid in Planetary Hydraulic Machines by Rational Design of Their Distribution Systems. *DSMIE 2022: Advances in Design, Simulation and Manufacturing V*. LNME. Springer, Cham, 2, 133-143 (2022). https://doi.org/10.1007/978-3-031-06044-1_13
7. Voloshina A, Panchenko A, Titova O, Panchenko I. Changes in the dynamics of the output characteristics of mechatronic systems with planetary hydraulic motors. Journal of Physics: Conference Series, 2021. Vol. 1741. 012045. https://doi.org/10.1088/1742-6596/1741/1/012045
8. Panchenko, A., Voloshina, A., Sadullozoda, S. S., Boltyansky, O., Panina, V.: Influence of the Design Features of Orbital Hydraulic Motors on the Change in the Dynamic Characteristics of Hydraulic Drives. *DSMIE 2022: Advances in Design, Simulation and Manufacturing V*. LNME. Springer, Cham, 2022. 2. 101–111. https://doi.org/10.1007/978-3-031-06044-1_10
9. Kiurchev S., Kyurchev V., Fatyeyev A., Tynyanova I., Mudryk K. Influence of the Radius of Curvature of the Teeth on the Geometric and Functional Parameters of the Rotors of the Planetary Hydraulic Motor. *Interpartner 2023: Advanced Manufacturing Processes V*. LNME. Springer, Cham, 2023. 450–461. https://doi.org/10.1007/978-3-031-42778-7_42.
10. Kiurchev S., Kyurchev V., Radkevych O., Fatyeyev O., Hrechka I. Monitoring the Accuracy of Manufacturing Elements of the End Distribution System of a Hydraulic Motor Planetary Type. *Interpartner 2024: Advanced Manufacturing Processes VI*. LNME. Springer, Cham, 2025. 712–723. https://doi.org/10.1007/978-3-031-82746-4_63
11. Wang Y., Shen T., Tan C., Fu J., Guo S. et al. Research Status, Critical Technologies, and Development Trends of Hydraulic Pressure Pulsation Attenuator. *Chinese Journal of Mechanical Engineering*. 2021. 34. 14. https://doi.org/10.1186/s10033-021-00532-z.
12. Eyres R. D., Champneys A. R., Lieven N. A. J. Modelling and Dynamic Response of a Damper with Relief Valve. *Nonlinear Dynamics*. 2005. 40 (2). 119–147. https://doi.org/10.1007/s11071-005-4144-6
13. Li D., Liu Y., Gong J., Wang T. Design of a Noncircular Planetary Gear Mechanism for Hydraulic Motor. *Mathematical Problems in Engineering*. 2021. 5510521. 1–9. https://doi.org/10.1155/2021/5510521
14. Panchenko, A., Voloshina, A., Fatyeyev A., Tynyanova I. and Mudryk K. Stabilization of the Transient Dynamic Characteristics for a Hydraulic Drive with a Planetary Hydraulic Motor. *DSMIE 2023: Advances in Design, Simulation and Manufacturing VI*. LNME. Springer, Cham, 2023. 2. 95–105. https://doi.org/10.1007/978-3-031-32774-2_10

15. Dasgupta K., Mandal S. K., Pan S. Dynamic analysis of a low speed high torque hydrostatic drive using steady-state characteristics. *Mechanism and Machine Theory*. 2012. 52. 1–17. https://doi.org/10.1016/j.mechmachtheory.2011.12.004

16. Zeman P., Kemmetmüller W., Kugi A. Mathematical Modeling and Analysis of a Hydrostatic Drive Train. *IFAC-PapersOnLine*. 2015. 48 (1). 508–513. https://doi.org/10.1016/j.ifacol.2015.05.064

17. Li C., Jiang T., Liu C., Xu H., Shi G. Investigation of the leakage in the flow distribution pair of radial piston hydraulic motors through CFD analysis and experiments. *Flow Measurement and Instrumentation*. 2024. 96. 102555. https://doi.org/10.1016/j.flowmeasinst.2024.102555

18. Kyurchev, V., Kiurchev, S., Rezvaya, K., Fatyeyev, A., Głowacki, S. Assessing the Reliability of a Mathematical Model of Working Processes Occurring in a Hydraulic Drive. *DSMIE 2024: Advances in Design, Simulation and Manufacturing VII*. LNME. Springer, Cham, 2024. https://doi.org/10.1007/978-3-031-63720-9_24

19. Ghoshal S. K., Pandey A. K , Dasgupta K., Bhola M. A segmental pump-motor control scheme to attain targeted speed under varying load demand of a hydraulic drive used in heavy earth movers. *Mechatronics*. 2021. 80. 102681. https://doi.org/10.1016/j.mechatronics.2021.102681

20. Gaheen O. A., Aziz M.A., Benini E. Experimental and modeled response of hydraulic motors under pulsating flow. *Engineering Science and Technology, an International Journal*. 2025. 72. 102234. https://doi.org/10.1016/j.jestch.2025.102234.

21. Fang Y., Yang H., Zhang G. et al.Multi-interface fusion speed pulsation model and behavior analysis for high-torque hydraulic motors. *Flow Measurement and Instrumentation*. 2026. 108. 103148. https://doi.org/10.1016/j.flowmeasinst.2025.103148

22. Grimaldi K., Najjaran A., Ma Z., Bao H., Roskilly T. Dynamic Modelling and Experimental Validation of a Pneumatic Radial Piston Motor. *Energies*, 2023. 16 (4). 1954. https://doi.org/10.3390/en16041954

23. Kojima E., Yamada T., Narikawa H., Moriyama K. A Simulation Model of the Delivery Flow Ripple produced by a Hydraulic Axial Piston Pump. *Transactions of the Japan Hydraulics & Pneumatics Society*. 1998. Vol. 29, No. 4. P. 100–106. https://doi.org/10.14888/jfps1998.29.100

24. Casoli P., Gherardini F., Campanini F. Active Pressure Ripple Control in Axial Piston Pumps through High-Frequency Swash Plate Oscillations – A Theoretical Analysis. *Energies*. 2019. 12 (7). 1377. https://doi.org/10.3390/en12071377.

25. Kojima E., Shinada M. Characteristics of Fluidborne Noise Generated by a Fluid Power Pump: 4th Report, Pressure Ripple in Hydrostatic Power Transmission. *Journal of the Japan Society of Mechanical Engineers*. 1986. 29 (258). 4147–4155. https://doi.org/10.1299/jsme1958.29.4147

26. Johnston D. N., Edge K. A. Simulation of the Pressure Ripple Characteristics of Hydraulic Circuits. *Proceedings of the Institution of Mechanical Engineers, Part I*. 1989. 203 (4). https://doi.org/10.1243/PIME_PROC_1989_203_114_02

27. Dindorf R., Takosoglu J., Wos P. Review of Hydro-Pneumatic Accumulator Models for the Study of the Energy Efficiency of Hydraulic Systems. *Energies*. 2023. 16 (18). 6472. https://doi.org/10.3390/en16186472.

28. Ray A. Dynamic modeling and simulation of a relief valve. *Simulation*. 1978. 31 (5). https://doi.org/10.1177/003754977803100504

29. Song W., Yang C. Mathematical Modelling and Dynamic Analysis of a Direct-Acting Relief Valve Based on Fluid-Structure Coupling Analysis. *Shock and Vibration*. 2021. 5581684. https://doi.org/10.1155/2021/5581684

30. Panchenko A. I., Voloshyna A. A., Rozhniatovskyi V. V., Zasiadko A. I. Model hidravlichnoho pryvodu mekhatronnoi systemy z planetarnym hidromotorom. *Promyslova hidravlika i pnevmatyka*, 2024. № 2(74). S. 12–32. https://doi.org/10.32782/1994-4691-2024-2-74-2

Дата першого надходження статті до видання 25.09.2026
Дата прийняття статті до друку після рецензування 21.10.2026
Дата публікації (оприлюднення) статті 04.11.2026
Стаття поширюється на умовах ліцензії відкритого доступу(CC BY 4.0)

ДИНАМІЧНА МОДЕЛЬ ГІДРАВЛІЧНОГО ПРИВОДУ МЕХАТРОННОЇ СИСТЕМИ З ПЛАНЕТАРНИМ ГІДРОМОТОРОМ

А. І. Панченко[1], А. А. Волошина[1], І. А. Панченко[1], І. М. Холод[1], А. А. Волошин[2]
[1] *Таврійський державний агротехнологічний університет імені Дмитра Моторного,*
[2] *ВСП «Мелітопольський фаховий коледж ТДАТУ»*

Анотація

У статті узагальнено результати розрахункових досліджень динамічних характеристик гідроприводу мехатронної системи із серійним і модернізованим планетарними гідромоторами. Мета роботи – зіставити вплив конструкції гідромотора, зовнішніх збурень і пасивного гасіння пульсацій на перехідні процеси гідроприводу. В аналізі враховано площу прохідного перерізу розподільної системи, діаметральний зазор між роторами, нерівномірність подачі насоса та зміну моменту опору. Розглянуто три випадки: постійні подача насоса й момент опору, змінні зовнішні впливи та робота з пасивним гасником пульсацій. Зміна площі прохідного перерізу розподільної системи супроводжується пульсаціями тиску й витрати робочої рідини, а зміна діаметрального зазору — коливаннями крутного моменту. За змінних зовнішніх впливів модернізований гідромотор характеризується меншими коливаннями тиску й крутного моменту та раніше досягає робочого рівня частоти обертання порівняно із серійним. У випадку застосування пасивного гасника пульсацій об’ємом 5000 см³ пускові максимуми тиску становлять приблизно 38 і 36 МПа для серійного та модернізованого гідромоторів відповідно, порівняно з 90 і 85 МПа без гасника. Пускові максимуми крутного моменту перебувають у межах 900–1000 Н·м для обох конструкцій, порівняно з приблизно 2100 і 1900 Н·м без гасника. Водночас коливання за змінного навантаження зберігаються в обох конструкцій. Результати обґрунтовують доцільність спільного розгляду конструктивного вдосконалення гідромотора та пасивного демпфування під час вибору заходів зі зменшення пульсацій і пускових навантажень. Числові оцінки стосуються розглянутих випадків з урахуванням відмінностей їхніх вихідних параметрів та умов роботи.

Ключові слова: перехідні процеси, розгін гідроприводу, тиск, крутний момент, витрата робочої рідини, частота обертання.

Conflict of Interest: The author is the journal’s editor-in-chief. To ensure the independence of the editorial process, the manuscript was handled by a designated editor who was not subordinate to the author and had no conflict of interest. The author did not participate in the selection of reviewers, the peer-review process, or the decision to publish the article. The manuscript underwent the standard double-blind peer review process.